Energy & Environmental Science

Cite this: *Energy Environ. Sci.*, 2012, **5**, 9698

www.rsc.org/ees

REVIEW

Liquid-phase chemical hydrogen storage materials

Mahendra Yadav and Qiang Xu*

Received 22nd July 2012, Accepted 18th September 2012
DOI: 10.1039/c2ee22937d

In the search for future energy supplies, the application of hydrogen as an energy carrier is seen as a prospective issue. However, the implementation of a hydrogen economy is suffering from several unsolved problems. Particularly challenging is the storage of appropriate amounts of hydrogen. In this context one of the promising hydrogen storage techniques relies on liquid-phase chemical hydrogen storage materials, in particular, aqueous sodium borohydride, ammonia borane, hydrazine, hydrazine borane and formic acid. The use of these materials in hydrogen storage provides high gravimetric and volumetric hydrogen densities, low potential risk, and low capital investment because it is largely compatible with the current transport infrastructure. In this review, we survey the research progresses in hydrogen generation from these liquid-phase chemical hydrogen storage materials and their regeneration.

1. Introduction

The ever-increasing demands of society put more-and-more stringent conditions on the efficiency of production, distribution and use of energy.[1] Society awaits a major technological breakthrough before we can reduce our overuse and dependence on fossil fuels that are rapidly depleting and causing serious damage to the planet. Thus, the development of clean alternative fuel sources based on renewable energy is the subject of recent attention. Hydrogen is one of the most promising candidates to replace nonrenewable fuel sources used nowadays because it is a renewable, environmentally friendly energy carrier, and in addition hydrogen has the greatest specific energy of any fuel directly fed into a PEM fuel cell; in fact, H_2 has twice as much specific energy as its closest competitor, methane.[2] There is no doubt that a great part of the world energy demands of this century will be fulfilled by hydrogen-based fuel cell technology.[3]

The establishment of a sustainable hydrogen-based energy future forces us to develop clean/renewable hydrogen production, efficient hydrogen storage and convenient distribution. The storage of large quantities of hydrogen at a low pressure is one of the key factors in establishing such a hydrogen-based economy.[4] In particular, for on-board energy storage, vehicles need compact, light, safe, and affordable hydrogen containment. Although liquid hydrogen has high gravimetric and volumetric hydrogen densities, it has several disadvantages, including its continuous boil-off, in particular for on-board storage. Compressed hydrogen gas is an alternative; high-pressure hydrogen-storage tanks up to 700 bar have been developed, which enables a vehicle driving range of ~300 miles.[4] Systems under higher pressures that could hold higher hydrogen densities are complicated by safety concerns and logistical obstacles. Other storage materials and methods,[5] including metal hydrides,[3,6] metal–organic frameworks,[7,8] on-board reforming of

National Institute of Advanced Industrial Science and Technology (AIST), Ikeda, Osaka 563-8577, Japan. E-mail: q.xu@aist.go.jp; Fax: +81 72 751 9629; Tel: +81 72 751 9562

Broader context

Hydrogen is foreseen to become a major energy carrier in the relatively close future. The shift towards a so-called hydrogen economy is driven by both a shortage in fossil fuels (while it seems possible to gain "green" hydrogen from renewable sources) and tremendous progresses in the production of fuel cells (making them suitable for transportation applications). A major problem to complete this shift is to find suitable ways to store hydrogen. Indeed, to be implemented at an industrial scale, storage devices must store as much hydrogen as possible within the smallest possible volume. Moreover, the storage as well as the release temperatures must be as close as possible to ambient conditions. Achieving such goals is proving to be a rather difficult task. Among the many possible systems, one of the promising hydrogen storage techniques relies on liquid-phase chemical hydrogen storage materials, in particular, aqueous sodium borohydride, ammonia borane, hydrazine, hydrazine borane and formic acid. In this review, we present a survey on the research progresses in catalytic hydrogen generation from these liquid-phase chemical hydrogen storage materials and their regeneration.

hydrocarbon into hydrogen,[9] and organic materials,[10,11] have also been investigated extensively. However, many of the candidate materials are still not able to meet the practical requirements such as volumetric (>82 $gH_2\ L^{-1}$) and gravimetric hydrogen capacities (>90 $gH_2\ kg^{-1}$), handling pressure and temperature, recycling of by-products, cost, and so on, for mobile applications.[4]

Chemical hydrogen storage which involves storing of hydrogen in the form of chemical bonds is one of the safe alternatives to physical hydrogen storage.[12] Over the past decades, solid-state hydrogen storage materials have received considerable attention as promising chemical hydrogen storage materials due to their attractive features, such as high hydrogen density, relative stability and safe storability.[12–14] There are many solid-state materials with high hydrogen storage capacities, which, however, display drawbacks, like the high temperature required to desorb hydrogen, slow hydrogen release kinetics or deterioration with successive cycling, different loading/unloading logistics and heat dissipation issues.[15] Thus, the search for safe and efficient liquid-phase hydrogen storage materials to conveniently release hydrogen under mild conditions is desired urgently. In this respect, hydrolysis of aqueous boron-based compounds, such as, $NaBH_4$, NH_3BH_3 and $N_2H_4BH_3$ has received much attention.[16–25] Recently, selective decomposition of hydrous hydrazine ($H_2NNH_2 \cdot H_2O$) to hydrogen and nitrogen at room temperature makes hydrazine a promising hydrogen carrier for storage and transportation.[26,27] In addition, formic acid, one of the major products formed in biomass processing, is non-toxic and a liquid at room temperature (density, 1.22 g cm^{-3}) containing 4.4% (w/w) of hydrogen, has also shown to be a potential hydrogen storage material.[28–30] This review discusses the state-of-the-art of these representative material systems for hydrogen storage, aiming at providing an outline of the forefront of catalytic hydrogen release and regeneration of the liquid-phase chemical hydrogen storage materials.

2. Sodium borohydride

2.1. Catalytic hydrogen generation from sodium borohydrides in liquid phase

Sodium borohydride ($NaBH_4$, SB) is one of the most studied chemical hydrides owing to its combined advantages of high hydrogen capacity (with a theoretical value of 10.8 wt%),[31] easy control of the hydrogen generation rate, friendly operation (low reaction-initiation temperature, stability in air under no pressure, and the $NaBH_4$ solution is nonflammable) and the environmentally benign hydrolysis product ($NaBO_2$ sodium metaborate).[31–33] Hydrogen stored in $NaBH_4$ can be released either by thermolysis[34,35] or by hydrolysis.[36–40] However, in a practical hydrogen generation system only the hydrolysis approach has been used. This is because in hydrolysis one-half of the hydrogen produced derives from water, resulting in a high hydrogen storage capacity. In addition, the generated H_2 has high purity (no CO, S) and is humidified (heat generates some water vapour), which facilitates its use in fuel cells. Hydrolysis is typically conducted in the aqueous phase at lower temperatures.

$NaBH_4$ undergoes hydrolysis at room temperature and liberates a theoretical hydrogen content of 10.8 wt% *via* the following reaction [eqn (1)].[33,36] Ideally, one mole of sodium borohydride reacts with 2 moles of water to liberate 4 moles of hydrogen.

$$NaBH_4 + 2H_2O \rightarrow NaBO_2 + 4H_2 \quad (1)$$

However, in real conditions hydrolysis reaction needs more water to release 4 moles of hydrogen because of the low solubility of both $NaBH_4$ and the borate byproducts in water. The use of excess of water lowers the theoretical gravimetric hydrogen storage capacity of $NaBH_4$; for example, the use of 4 moles of water results in a hydrogen content of 7.3 wt% in comparison to the use of 2 moles of water [eqn (1)], which corresponds to a hydrogen content of 10.8 wt%.[25,38]

Mahendra Yadav

Mahendra Yadav was born in Kushinagar, U. P., India in 1984. He received his MSc in Chemistry from Deen Dayal Upadhyay Gorakhpur University, India in 2006 and PhD degree in Inorganic Chemistry under the supervision of Prof. D. S. Pandey from Banaras Hindu University, Varanasi, India in 2010. He then joined Prof. Qiang Xu's group at AIST as a JSPS (Japan Society for the Promotion of Science) postdoctoral fellow in 2010. He is currently interested in development of homo-/heterogeneous catalysts for the activation of small molecules for chemical hydrogen storage.

Qiang Xu

Qiang Xu received his PhD degree in Physical Chemistry in 1994 at Osaka University, Japan. After one year working as a postdoctoral fellow at Osaka University, he started his career as a Research Scientist in Osaka National Research Institute in 1995. Currently, he is a Senior Research Scientist at the National Institute of Advanced Industrial Science and Technology (AIST, Japan) and adjunct professor at Kobe University. He received the Thomson Reuters Research Front Award in 2012. His research interests include porous and nanostructured materials and related functional applications, especially for clean energy. He has published more than 250 papers in refereed journals.

Hydrolysis is thermodynamically favored and is a very exothermic process. $NaBH_4$ undergoes self-hydrolysis (hydrolysis without catalyst) in aqueous solution. However, aqueous phase reactions with pure water give very slow hydrogen generation, because after some initial hydrolysis the reaction mixture becomes basic and the reaction intermediates are stabilized at elevated pH. This allows the use of bases as stabilizers to prevent premature reaction and acids as catalysts to improve the kinetics of sodium borohydride hydrolysis.[31,33] In addition, metal catalysts have also been found to catalyze the hydrolysis reaction.[33,36,37,41–43]

These two catalytic approaches (use of acid additives or the use of metal catalysts) have been widely investigated to improve the hydrolysis rate of the sodium borohydride reaction.[31,33,36–44] Early in the 1950s, Schlesinger *et al.* reported acid-catalyzed hydrolysis of $NaBH_4$ at ambient conditions.[33] It was observed that in the presence of acid, $NaBH_4$ solution released 90% of the stoichiometric amount of hydrogen from the hydrolysis reaction. However, this technique requires large amounts of acid, making this method unsafe, heavy and bulky. The difficulty of controlling the reaction is a further drawback. Because of this, the use of acid as a catalyst for $NaBH_4$ hydrolysis has not been considered as a potential accelerator for hydrogen release. However, the effect of acid accelerators on hydrogen generation from solid sodium borohydride for small-scale portable applications has been studied. Prosini and Gilson designed a hydrogen generator for a fuel cell powered cellular phone based on the "hydrogen on demand" concept and taking advantage of the hydrolysis of solid $NaBH_4$ with HCl–water solution.[44] They also evaluated the optimum HCl–hydride (= 1), HCl–H_2O (= 1.6), and acid solution–boride (= 3.6 cm^3 g^{-1}) ratios and hydrogen mass flow rates upon operation. Murugesan and Subramanian also studied hydrogen generation using acidified water and solid $NaBH_4$ for small-scale portable applications.[45] They investigated various acids (mineral acids: HCl, H_2SO_4, HNO_3, H_3PO_4; organic benign acids: HCOOH, CH_3COOH) on hydrogen yield from solid $NaBH_4$. With all the mineral acids studied, they observed an increase in the hydrogen production rate, which increased with increasing acid concentration. In the case of benign organic acids, higher concentrations, in general, are required to provide hydrogen production rates similar to those with mineral acids.

Since Schlesinger *et al.*[33] found the $NaBH_4$ hydrolysis by acids, few investigations on homogeneous catalysts have been carried out due to the difficulty of the control of the reaction process. Recently, Keçeli and Özkar suggested using ruthenium(III) acetylacetonate as the homogeneous catalyst for the $NaBH_4$ hydrolysis reaction.[46] A number of heterogeneous catalysts based on metals or metal compounds or metal alloys have been reported to be active for catalytic hydrolysis of sodium borohydride in alkaline solutions under ambient conditions, including Co, Ni, Fe, Ru, Pt, Pd, Ru–Cu, Ru–Pd, Ru–Ag, Ru–Pt, Pt–Ag *etc.*[33,47–62] The efficiency of the catalyst has been investigated in terms of the type and form of the catalyst.[54,55]

Initially, noble metal catalyzed hydrolysis of $NaBH_4$ was investigated by using metal salts *e.g.* $RuCl_3$, $RhCl_3$, H_2PtCl_6, $IrCl_4$, $PdCl_2$ *etc.* Among them $RuCl_3$, $RhCl_3$, H_2PtCl_6 were found most active, and during the hydrolysis reaction these metals are reduced to the elementary state.[33,41] After that Amendola *et al.* reported Ru catalyst supported on ion exchange resin beads which show high activity for hydrolysis of $NaBH_4$.[36,37] They investigated the effects of $NaBH_4$, NaOH concentrations and temperature on the rate of the hydrolysis reaction. Ru metal supported on anionic resins showed better activities than cationic resins. The A-26 and IRA-400 anion exchange resins gave the highest hydrogen generation rates. They claimed that the slow rate at the beginning with high concentrations of $NaBH_4$ was due to the high viscosity of the solution. Further, it was observed that high concentrations of hydroxyl ions from NaOH decreased water molecules available for hydrolysis reaction. Demirci and Garin investigated the activity of different alloy based catalysts and the activity decreased in the order Ru, Ru_2Pt_1 > RuPt, Ru_1Pt_2 > RuPd > RuAg, Pt > RuCu > PtAg.[52] Kojima *et al.* reported the first study dealing with transition metals supported on various oxides (Co_3O_4, TiO_2, SiO_2, NiO, $LiMn_2O_4$, TiO, CoO, Ti_2O_3, $LiNiO_3$ and $LiCoO_2$).[43] The 1.5 wt% Pt/$LiCoO_2$ catalyst showed the best performance. A hydrogen generation rate higher than 200 $L(H_2)$ min^{-1} g^{-1} (Pt) was observed and it was claimed that this rate was ten times faster than the Ru catalyst reported by Amendola *et al.*[36,37] Krishnan *et al.* alloyed Pt to Ru and compared 10 wt% Pt–Ru/$LiCoO_2$ to both 10 wt% Ru/$LiCoO_2$ and 10 wt% Pt/$LiCoO_2$. The efficiency of Pt–Ru/$LiCoO_2$ was almost double of that of the Ru- and Pt-based catalysts.[67] Later, Yang and coworkers tested various supports for dispersing Pt–Ru: *e.g.* Co_3O_4, NiO, $LiCoO_2$, $LiNiO_2$, $LiMnO_2$, TiO_2 and ZrO_2. The best catalytic systems were Pt–Ru/Co_3O_4 followed by Pt–Ru/$LiCoO_2$.[64] Zeolite-confined ruthenium(0) nanoclusters catalyst with turnover frequency (TOF) up to 33 000 h^{-1} have been reported by Zahmakiran and Özkar.[65] In general, noble metals show high activity in comparison with non-noble metals.

Non-noble metal catalysts, especially nickel and cobalt, are attractive because of their low-cost and comparable catalytic activity. As a result, improvement of the hydrogen generation activity of the low-cost catalyst is becoming imperative and necessary. In the beginning, a number of non-noble metal salts (manganese, iron, cobalt, nickel and copper chlorides) were tested and results show that Co and Ni metal based catalysts were the most active.[33,41] Typically it was observed that the salts reacted rapidly with $NaBH_4$ solutions and gave finely divided black precipitates of metal borides. Accordingly, metal borides like cobalt or nickel borides have been prepared by the chemical reduction method using $NaBH_4$ as a reduction chemical and their catalytic activity has been investigated by many groups.[54,60,66,67] In addition, Wu *et al.* heat-treated the obtained CoB at various temperatures.[67] It was observed that the catalyst treated at 500 °C exhibited the best catalytic activity because it had the best crystallisation (the more crystallised, the more active). Liu *et al.* compared the catalytic activity of Co_2B to those of cobalt powder, cobalt chloride and RANEY® cobalt. Co_2B [468 $mL(H_2)$ min^{-1} g^{-1} (Co_2B)] was better than the powder [126 $mL(H_2)$ min^{-1} g^{-1} (Co)] and the RANEY® [268 $mL(H_2)$ min^{-1} g^{-1} (Co)] but was less active than the cobalt chloride [570 $mL(H_2)$ min^{-1} g^{-1} (Co_2B)].[59] Patel *et al.* used CoB-based thin film catalyst synthesised by a pulsed laser deposition technique which permitted the formation of CoB nanoparticles (NPs).[68,69] It was observed that cobalt was efficient only when alloyed with boron, which partially prevents metal oxidation. Hanxi and coworkers claimed the preparation of a highly stable

and active nickel boride catalyst (Ni_xB), even if its performance was four times lower than that of a Ru-based catalyst at room temperature.[70] Furthermore, it has been reported that the structure and catalytic activity of the produced catalyst are generally sensitive to its preparation conditions. The conditions include the type of reducing agent,[62] the pH of the reduction medium during the preparation of the catalyst,[36,59] the type of precursor and phase of the precursor,[71,72] the ratio of reducing ion–metal ion,[73] and heat treatment.[73,74] Performances of some selected catalysts are summarized in Table 1.

In addition to hydrolysis, the hydrogen generation from $NaBH_4$ in other solvents, like alcohols, was also assessed.[82–84] $NaBH_4$ is known to be reactive to *e.g.* methanol and ethanol and methanol has the highest reactivity towards $NaBH_4$.[82,83] The overall reaction between methanol and $NaBH_4$ can be described as [eqn (2)]:

$$NaBH_4 + 4CH_3OH \rightarrow NaB(OCH_3)_4 + 4H_2 \quad (2)$$

Karan and coworkers assessed the H_2 generation in methanol and mixtures of methanol and water ($H_2O/NaBH_4$ molar ratio of either 2 or 10).[82] The best system was the mixture with a molar ratio of 10. Demirci and coworkers investigated metal catalyzed methanolysis by using Co/TiO_2 and Ru/TiO_2 catalysts. Co/TiO_2 shows high catalytic performances, higher than that of $Ru–TiO_2$. Hydrogen generation rates of 144 to 644 $L(H_2)\ min^{-1}\ g^{-1}$ (Co) were measured as the Co loading on TiO_2 was decreased from 20 to 1 wt%.[85]

2.2 Regeneration of sodium borohydride

For $NaBH_4$ to be used as a viable hydrogen fuel, an economical and environmentally sound process for recycling of spent fuel to $NaBH_4$ is needed. In the hydrolysis of $NaBH_4$, it has been reported that BH_4^- transforms to $B(OH)_4^-$,[86,87] and at pH < 9, $B(OH)_3$ is the predominant byproduct in aqueous solutions, whereas at pH > 9, mainly $B(OH)_4^-$ forms.[31] However, upon drying at <110 °C, the species present are primarily $NaBO_2 \cdot 2H_2O$ and $NaBO_2 \cdot 4H_2O$.[88] The formation of $Na_2B_4O_7 \cdot 5H_2O$ has also been reported.[89] At higher drying temperatures, the hydrated borates dehydrate to form, for example, $NaBO_2 \cdot 1/2H_2O$ and then $NaBO_2$.[88] Considerable efforts have been devoted to find a suitable route to prepare $NaBH_4$ from $NaBO_2$. The borate species are thermodynamically stable,[31] thus requiring a large quantity of energy to regenerate the parent material. This is one major demerit which limits the on-board vehicular applications of $NaBH_4$.[90,91] In general, the recycling process of byproducts formed by hydrolysis of $NaBH_4$ involves the separation of borates from unreacted $NaBH_4$ of the reaction slurry and then drying at temperatures of approximately 300 °C to obtain anhydrous $NaBO_2$.[92,93] The as-obtained $NaBO_2$ can then be transformed back into $NaBH_4$ by several reported processes.[94,95] Some notable $NaBH_4$ preparation processes are briefly discussed here.

The Bayer process has been employed for commercial scale synthesis of $NaBH_4$. In this process $NaBH_4$ was prepared by the reaction of borax ($Na_2B_4O_7$), metallic sodium (Na), hydrogen (H_2) and silica (SiO_2) at high temaparture.[96] This process was further modified by employing less expensive reducing metal magnesium instead of sodium. The modified Bayer process is a one-pot synthesis of sodium borohydride by reduction of $NaBO_2$ using magnesium (Mg)[97,98] or magnesium hydride (MgH_2)[99,100] as a reducing agent [eqn (3)]. Although this employed the less expensive reducing metal, high yields and fast reaction rates could not be achieved. Theoretically, the reaction could occur at room temperature in accordance with the standard Gibbs free energy ($\Delta G^0 = -269.7\ kJ\ mol^{-1}$). However, the investigators found that the process should be carried out at high temperature because of poor mass transfer between the solid particles of the reactants, as well as high hydrogen pressure providing MgH_2 decomposition at high temperatures.

$$NaBO_2 + 2MgH_2 \rightarrow NaBH_4 + 2MgO \quad (3)$$

It was reported that $NaBH_4$ produced from the modified Bayer process is in molten form and does not decompose at 550 °C and 7 MPa (under hydrogen atmosphere) for 2 h.[98] Because the modified Bayer process needs to be conducted under severe reaction conditions with hazardous materials, it is a high-risk process, especially if one contemplates a large-scale industrial production. Furthermore, an effective method to separate the reaction products is required to obtain a reasonable yield of $NaBH_4$.[94]

A one-step synthetic approach should be desirable *e.g.*, using the direct thermal reduction of sodium borate by a reducing agent such as, methane (or natural gas), H_2 or carbon. However, investigations of free energies of the reactions indicated that they are not thermodynamically feasible under reasonable conditions.[94,101]

While developing an all-thermal synthetic process for $NaBH_4$, Millenium Cell Inc. proposed a family of processes[102–105] which can be modified in various ways to optimize the tradeoffs among energy efficiency, cost and greenhouse gas emissions. One example is based on the use of disproportionation, a classic reaction in the chemistry of boron compounds.[106] Another

Table 1 Performances of selected catalysts for hydrogen generation from hydrolysis of sodium borohydride[a]

Catalyst	HGR ($L(H_2)\ min^{-1}\ g^{-1}$)	T (°C)	Ref.
$CoCl_2$	11.4	20	89
CoB	2.8	30	60
CoB–Ni	11.0	30	75
CoWB–Ni	15.0	30	76
CoP–Cu	1.0	30	77
Ru	4.0	25	37
$Ru_{60}Co_{40}$	17.5	25	78
$Ru_{80}Fe_{20}$	18.3	25	78
$Ru_{60}Co_{20}Fe_{20}$	26.8	25	78
10 wt% $Ru/LiCoO_2$	428	25	63
1.5 wt% $Pt/LiCoO_2$	203	22	43
10 wt% $Pt/LiCoO_2$	300	25	63
10 wt% $PtRu/LiCoO_2$	560	25	63
10 wt% Ru/CF	14.2	20	78
20 wt% Pt/C	115	20	79
9 wt% $Co/\gamma Al_2O_3$	1	30	80
2 wt% $Ru/\gamma Al_2O_3$	4.8	30	81
16.6 wt% $Ru_{60}Co_{20}Fe_{20}$/CF	41.7	20	78
13.3 wt% $Ru_{75}Co_{25}$/CF	37.1	20	78

[a] HGR = hydrogen generation rate, CF = carbon fibres.

proposed carbon-based reduction method is based on formaldehyde as a reducing agent.[107]

An electrolytic process, which was first proposed by Cooper,[108] was thought of as the most attractive process for $NaBO_2$ recycling. The electrolytic reaction [eqn (4)] was carried out in the $NaBO_2$ caustic solution.

$$\begin{aligned}&\text{Anode reaction}: \ 4H_2O \rightarrow 2O_2 + 8H^+ + 8e\\&\text{Cathode reaction}: \ BO_2^- + 6H_2O + 8e \rightarrow BH_4^- + 8OH^-\\&\text{Total reaction}: \ NaBO_2 + 2H_2O \rightarrow NaBH_4 + 2O_2\end{aligned} \quad (4)$$

The plenty of OH^- in caustic solution could be electrolyzed prior to BO_2^-, and thus, the electrolysis of BO_2^- to BH_4^- in aqueous media proved to be difficult, if not impossible. Traces of $NaBH_4$ were detected in the products resulting from the electrosynthesis in aqueous media and it is suggested that this embryonic study should be pursued.[109] Calabretta and Davis and Calabretta[110] demonstrated an anhydrous molten Na–B–O–H system, which could be used as a potential medium in the electrolysis of BO_2^- to BH_4^-. This process is currently under investigation.[110]

At present, none of these processes is sufficiently simple to lower the cost of borohydride manufacture below its current level. Based on the current scenario of $NaBH_4$ synthesis, the most attractive route to achieving the low-cost production of sodium borohydride lies with the electrochemical methods, which, however, need to be realized.

2.3 Conclusions

Apart from its established use for hydrogenation and reduction processes in the chemical industry, sodium borohydride ($NaBH_4$) has been demonstrated as an effective hydrogen storage material. Its hydrolysis generates high purity humidified hydrogen suitable for use in PEM fuel cells. Although the technology can be scaled and tailored for many different applications from very small portable devices to fuel cell vehicles, the current high cost of $NaBH_4$ is limiting early adoption of the technology to premium power applications. The utilization of $NaBH_4$ in high demand, continuous power generation and fuel cell vehicles will not be economically feasible until the production cost of $NaBH_4$ can be significantly reduced. A substantial decrease in the $NaBH_4$ cost might be achieved by finding an effective method of recycling $NaBO_2$ back to $NaBH_4$, if possible, in electrochemical way.

3. Ammonia borane

3.1 Catalytic hydrogen generation from ammonia borane in liquid phase

Ammonia borane (NH_3BH_3, AB) has a hydrogen capacity of 19.6 wt%, exceeding that of gasoline and making it an attractive candidate for chemical hydrogen-storage applications.[16–23,111–116] It possesses a volumetric density of 146 $gH_2\ L^{-1}$ and a gravimetric density of 196 $gH_2\ kg^{-1}$. These values are well above the US Department of Energy targets (2015) of a volumetric density greater than 82 $gH_2\ L^{-1}$ and a gravimetric density greater than 90 $gH_2\ kg^{-1}$.[117] AB is a colorless molecular crystal at room temperature[118] with a density of 0.74 $g\ cm^{-3}$.[119] It is stable in air, and soluble in water and other relatively polar solvents.[21,120] Several methods have been developed for laboratory-scale preparation of AB, including reaction of ammonium salts with lithium or sodium borohydride,[119,121–123] and direct reaction of ammonia with diborane (B_2H_6),[124] $BH_3{\cdot}THF$[125] or $BH_3{\cdot}SMe_2$.[126] According to the literature reports, the most efficient one involves the reaction of $NaBH_4$ and ammonium formate (HCO_2NH_4) in dioxane, which gives high purity (≥98%) AB in high yield (≥95%).[123]

Ammonia borane is hydrogen-dense and thus mainly attractive for portable and automotive applications, and the primary challenge is to recover as much H_2 as possible and, where possible, under mild conditions (<85 °C). Release of hydrogen from AB can be accomplished either by thermolysis (neat or metal catalyzed) in the solid state and nonaqueous medium (ethereal solvents) or metal catalyzed reactions in protic solvents (water and methanol).[16–23,111–116]

To date, considerable works involving the release of hydrogen from the thermal dehydrogenation of AB have been reported.[112,113,127–130] Thermolysis is a three-step process [eqn (5)–(7)]. The first step commences at approximately 100 °C and releases 1 equiv. of H_2 (6.5 wt%). The second step occurs at a broad temperature range centered at approximately 150 °C. The final step, which requires high temperatures (>1200 °C), provides the third equivalent of H_2. Unwanted gaseous byproducts, such as borazine ($B_3N_3H_6$), are also liberated.[131] To reduce the threshold temperature and volatile byproducts, various approaches have been considered, including nano-scaffolding,[132] catalysis,[133,134] dispersion in an ionic liquid,[127] and the synthesis of derivatives (*e.g.*, amidoboranes).[129]

$$NH_3BH_3 \rightarrow 1/n[NH_2{-}BH_2] + H_2 \quad (5)$$

$$1/n[NH_2{-}BH_2] \rightarrow 1/n[NH{-}BH]_n + H_2 \quad (6)$$

$$1/n[NH{-}BH]_n \rightarrow BN + H_2 \quad (7)$$

Hydrogen release from AB is exothermic while the complete release of hydrogen needs high temperature. A conceptually different approach was conceived for the solvolysis of AB, mainly hydrolysis[16,17,135–138] and methanolysis,[123,139,140] where H_2 is released at ambient temperatures in the presence of suitable catalysts. The $H^{\delta-}$ bound to the B atom reacts with the $H^{\delta+}$ provided by the solvent. AB is highly soluble and quite stable in these media. The ^{11}B NMR spectrum remains unchanged in water for more than 80 days under an argon atmosphere, indicating the high stability of AB in water.[16,111] The aqueous medium should either be neutral or weakly basic for AB to be stable,[141] in a strongly basic medium AB is unstable.[142] The hydrolysis of AB occurs at an appreciable rate only in the presence of a suitable catalyst at ambient temperature, thus one of the major obstacles of the practical application of this system is to develop efficient, economical and easily recyclable catalysts for improving the kinetic properties under moderate conditions. The hydrolysis reaction can be briefly expressed as follows [eqn (8)]:[16]

$$NH_3BH_3 + 2H_2O \rightarrow NH_4^+ + BO_2^- + 3H_2 \quad (8)$$

A variety of Lewis and Brønsted acids,[21] solid and gaseous acids,[135] zeolites,[135] and even CO_2,[135] are efficient catalysts for the

Table 2 Hydrogen generation from aqueous NH_3BH_3 catalyzed by noble and non-noble metals

Catalyst	Catalyst/AB molar ratio (mol mol^{-1})	Maximum H_2/NH_3BH_3 ratio (mol mol^{-1})	Time for reaction completion (min)	Ref.
2 wt% Ru/γ-Al_2O_3	0.018	3.0	3	143
2 wt% Rh/γ-Al_2O_3	0.018	3.0	1.3	143
[Rh(1,5-COD)(μ-Cl)]$_2$	0.018	2.6	15	16
2 wt% Pd/γ-Al_2O_3	0.018	2.9	120	143
Pd black	0.018	2.6	250	16
2 wt% Pt/γ-Al_2O_3	0.018	3.0	0.8	143
2 wt% Pt/C	0.018	3.0	1.5	16
2 wt% Pt/SiO_2	0.018	3.0	3	143
PtO_2	0.018	3.0	8	16
Pt black	0.018	3.0	12	16
2 wt%Au/γ-Al_2O_3	0.018	1.9	610	143
Laurate stabilized Rh(0)	0.0025	3.0	6	138
Laurate stabilized Ru(0)	0.00125	3.0	22	144
Zeolite stabilized Rh(0)	0.004	3.0	67	146
10 wt% Co/γ-Al_2O_3	0.018	2.9	70	17
10 wt% Co/SiO_2	0.018	2.9	70	17
10 wt% Co/C	0.018	2.9	55	17
10 wt% Ni/γ-Al_2O_3	0.018	2.9	65	17
10 wt% Cu/γ-Al_2O_3	0.018	2.9	590	17
10 wt% Fe/γ-Al_2O_3	0.018	—[a]	—[a]	17
In situ synthesized Fe particle	0.12	3.0	8	148
Ni in starch	0.1	3.0	6	149
Bare Ni NPs	0.1	2.8	11	150
PVP–Ni NPs	0.1	2.7	9	150
$Fe_{0.5}Ni_{0.5}$	0.12	3.0	2.2	151
In situ synthesized Co	0.04	3.0	1.7	155

[a] No reaction.

hydrolysis. The performances of several metal-based hydrolysis catalysts are summarized in Table 2. Noble metal-based catalysts were firstly found by us to have considerable activities toward hydrolytic dehydrogenation of AB.[16] The Pt-based catalysts were reported to have high activity toward this reaction with the released H_2 to AB ratio up to 3.0 (Fig. 1) and the catalytic activities are in the order of 20 wt% Pt/C > 40 wt% Pt/C > PtO_2 > Pt black > K_2PtCl_4. The 20 wt% Pt/C catalyst shows the highest activity and the reaction is completed in less than 2 min (Pt/AB = 0.018).[16] In contrast, [Rh(1,5-COD)(μ-Cl)]$_2$ and Pd black have lower activity and some noble metal oxides (RuO_2, Ag_2O, Au_2O_3, IrO_2) are almost inactive.[16] The Ru, Rh, Pd, Pt and Au

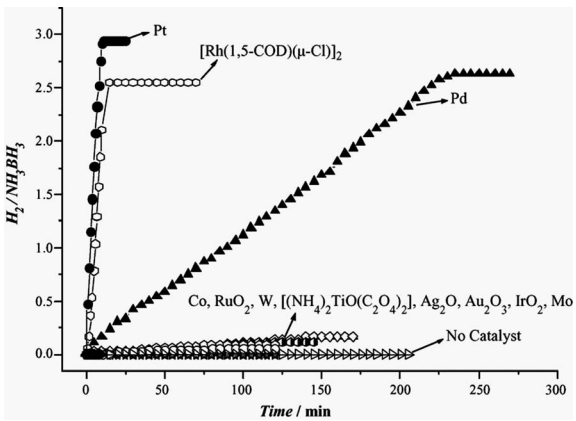

Fig. 1 Hydrogen release from aqueous NH_3BH_3 (0.33 wt%) solution in the presence of various metal catalysts (metal/NH_3BH_3 = 0.018). Reprinted with permission from ref. 16. Copyright 2006 Elsevier.

NPs supported on different supports (γ-Al_2O_3, VULCAN® carbon and SiO_2) were also investigated for hydrolysis of AB by our group.[143] It has been found that the Ru, Rh and Pt catalysts exhibit high activities to generate a stoichiometric amount of hydrogen with fast kinetics, whereas the Pd and Au catalysts are less active. In order to achieve well dispersed noble metal clusters/NPs with small sizes and study their kinetics, Özkar and co-workers have recently used different polymers (laurate or poly(4-styrenesulfonic acid-co-maleic acid)(PSSA-*co*-MA)) as stabilizers for metal NPs (Rh, Ru, Pd).[138,144,145] The resulting catalysts show significant enhancement in activity. Furthermore, they also investigated the catalytic activities of zeolite-Y confined Rh and Pd NPs,[146,147] which show high catalytic activities (TOF = 92 min^{-1} for Rh NPs) and long lifetime (47 200 turnovers for Rh NPs and 15 600 turnovers for Pd NPs) in the hydrolysis of AB at 25 °C.

Although the noble metal-based catalysts show very high activities for hydrolysis of AB as mentioned above, from the viewpoint of practical application, the development of efficient, low-cost, and stable catalysts to improve further the kinetic properties under moderate conditions is very important. As shown in Table 2, supported non-noble metal (Ni or Co) catalysts exhibit high activities, with which hydrogen is released in an almost stoichiometric amount from aqueous NH_3BH_3, and the reaction can be completed in 55–70 min (metal/NH_3BH_3 = 0.018), whereas supported Fe is catalytically inactive.[17] Afterwards, we systematically investigated the catalytic activities of unsupported first-row transition metal NPs, which were pre-reduced by $NaBH_4$ or *in situ* reduced in the presence of AB and $NaBH_4$ during the hydrolysis reaction. It is found that the catalytic activities are highly dependent on their particle sizes, crystallinities, compositions, *etc.*[148–153] Most importantly,

amorphous Fe NPs prepared by *in situ* reduction with AB/$NaBH_4$ were found to have an excellent catalytic activity for the hydrolysis of aqueous NH_3BH_3 under argon and even in air at room temperature, releasing hydrogen of $H_2/NH_3BH_3 = 3.0$ in *ca.* 8 min (Fe/AB = 0.12) (Fig. 2).[148] In addition, the amorphous Co and Ni and Fe–Ni alloy nanoparticles also exhibit much better catalytic activity than their crystalline ones.[149,151,154]

The $M@SiO_2$ nanospheres (M = Co, Ni) prepared with the reversed micelle method were found to have higher catalytic activity for hydrolysis of AB to generate a stoichiometric amount of H_2 compared to the M/SiO_2 nanosphere and Ni/commercial SiO_2 catalysts, which were synthesized by depositing Ni or Co NPs on SiO_2 nanospheres and commercial SiO_2, respectively, with the impregnation method.[152,155] Monodisperse nickel NPs supported on the Ketjen carbon support, synthesized by the reduction of $Ni(acac)_2$ with borane tributylamine (BTB) in the presence of oleylamine (OAm) and oleic acid (OA), were reported to exhibit high catalytic activity in hydrogen generation from the hydrolysis of the AB even at low catalyst and substrate concentrations at room temperature.[156] In a recent report by Song, Cai and coworkers, nanoporous Ni spheres showed a high activity with a TOF value 19.6, which was the highest among all the Ni-based catalysts and was about one fourth of the activity of the Pt catalyst (Fig. 3). Furthermore, the stability of these catalysts was improved by silica coating of the Ni spheres.[157]

Li and co-workers employed a Ni based metal–organic framework (MOF) as precursor for preparing a mixture of Ni NPs with undegradated Ni–MOF reduced by AB in methanol. The mixture exhibits a high catalytic activity for complete hydrogen generation from aqueous AB solution at 25 °C in air.[153] This group also reported a highly active Co(0) catalyst, synthesized by the $NaBH_4$ reduction of a metal–organic framework (MOF) precursor $Co_2(bdc)_2(dabco)$ (bdc = 1,4-benzenedicarboxylate; dabco = 1,4-diazabicyclo[2.2.2]octane), for the hydrogen generation from AB.[158] In the presence of the Co-MOF based catalyst, the hydrogen generation from aqueous AB solution (0.32 M) was completed within 1.4 min (MOF/$NaBH_4$/AB = 0.057/0.08/1) at room temperature.

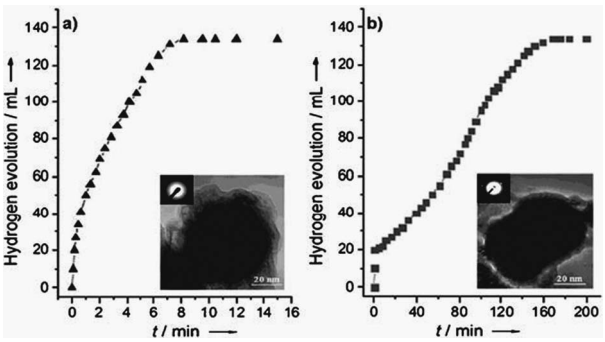

Fig. 2 Hydrogen generation by hydrolysis of aqueous AB (0.16 M, 10 mL) in the presence of (a) *in situ* synthesized Fe catalysts and (b) the pre-synthesized (Fe/AB = 0.12) at room temperature under argon. The volume of released gas includes 20 mL H_2 from the reducing agent $NaBH_4$, the volume of 1 equiv. $H_2 = \sim 59$ mL, 2 equiv. $H_2 = \sim 97$ mL, 3 equiv. $H_2 = \sim 136$ mL. Inset: TEM micrographs and the corresponding SAED patterns of the Fe NPs. Scale bar: 20 nm. Reprinted with permission from ref. 148. Copyright 2007 Wiley-VCH.

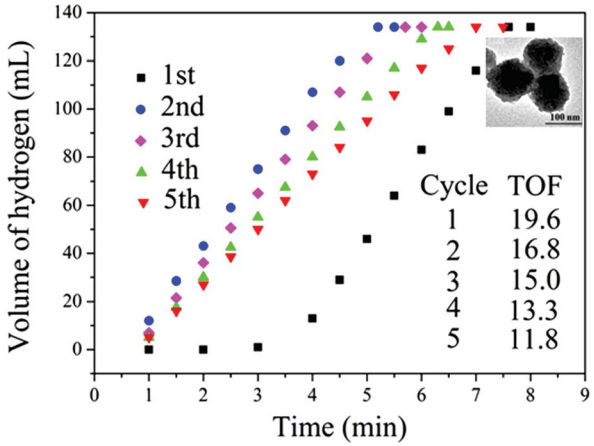

Fig. 3 Time *versus* volume of hydrogen generated from hydrolysis of AB catalyzed by nanoporous Ni spheres and corresponding TOF values up to five cycles. Volume of 1 equiv. $H_2 = \sim 48$ mL, 2 equiv. $H_2 = \sim 95$ mL, 3 equiv. $H_2 = \sim 142$ mL. Insect: TEM image of nanoporous Ni sphere catalyst. Reprinted with permission from ref. 157. Copyright 2010 Wiley-VCH.

Recently our group reported highly dispersed and small sized Ni NPs (~2.7 nm) immobilized by the frameworks of ZIF-8, which exhibit highly catalytic activity and durability for hydrolysis of ammonia borane (AB).[159] Among the samples, the sample prepared by using the chemical vapor deposition (CVD) approach (CVD–Ni@ZIF-8) showed the highest activity, with which the reaction can be completed ($H_2/AB = 3.0$) in 13 min (Ni/AB = 0.016), giving a TOF value of 14.2 min^{-1} in comparison to the sample prepared by using a chemical liquid deposition (CLD) approach (CLD–Ni@ZIF-8), with which the reaction can be completed in 19 min (Ni/AB = 0.019), giving a TOF value of 8.4 min^{-1}.

The copper nanoparticles synthesized using the Solvated metal atom dispersion (SMAD) method has been employed for the hydrolysis of ammonia borane. Controlled oxidation of the as-prepared nanoparticles resulted in the formation of $Cu@Cu_2O$ core–shell nanoparticles. The $Cu@Cu_2O$ core shell and Cu_2O NPs show better activities than pure Cu NPs for the generation of hydrogen in the AB hydrolysis reaction.[139] Zeolite confined Cu NPs were prepared by the ion-exchange of Cu^{2+} ions with the extra framework Na^+ ions in zeolite-Y followed by reduction of the Cu^{2+} ions within the cavities of zeolite with $NaBH_4$ in aqueous solution. Zeolite confined Cu NPs are active in the hydrolysis of AB with an average TOF value of 46.5 h^{-1} and provide 1300 turnovers in the catalytic hydrolytic dehydrogenation of AB.[160]

Bimetallic catalysts usually show enhanced catalytic performance in comparison to their monometallic counterparts. Various bimetallic (Ni–Fe, Ni–Au, Ni–Ag, Ni–Pt, Ni–Pd) catalysts have also been employed in the AB hydrolysis reaction.[151,161] These catalysts show superior catalytic activity due to a synergistic effect in comparison to their monometallic counterparts. Recently, we have prepared Au–Ni and Au–Co NPs with small diameters (3–4 nm) within silica nanospheres (around 15 nm) by using $Au(en)_2Cl_3$, $Ni(NH_3)_6Cl_2$ and $Co(NH_3)_6Cl_2$ as precursors in a NP-5/cyclohexane reversed-micelle system, followed by *in situ* reduction in an aqueous solution of $NaBH_4$/AB.

Compared with monometallic $Au@SiO_2$, $Ni@SiO_2$ and $Co@SiO_2$ counterparts, the $Au–Ni@SiO_2$ and $Au–Co@SiO_2$ catalysts exhibit superior performances in the hydrolytic dehydrogenation of AB.[162,163] The synergistic effect between Au and Ni or Au and Co inside the silica nanospheres plays an important role in the catalytic hydrolysis of NH_3BH_3. Furthermore, we have also investigated the effect of heat treatment of core–shell structured $Au–Co@SiO_2$ nanospheres. During heat treatment in vacuum, it has been observed that multiple Au–Co NPs embedded in SiO_2 nanospheres ($Au–Co@SiO_2$–RT) merged into single Au–Co NPs in SiO_2 ($Au–Co@SiO_2$–HT), resulting in a size increase of the Au–Co NPs. The $Au–Co@SiO_2$–HT nanospheres showed better catalytic activity than the $Au–Co@SiO_2$–RT. The higher catalytic activity of $Au–Co@SiO_2$–HT could be attributed to the decrease in the content of basic ammine by the decomposition of metal ammine complexes during the heat treatment.

Similar to alloy NPs, core–shell structured bimetallic NPs are also very important for catalytic applications. Recently, our group prepared magnetically recyclable Au@Co core–shell NPs by a rational and general strategy through the one-step seeding-growth route with AB as the reducing agent under ambient conditions.[164] Au NPs can be formed first, and serve as the *in situ* seeds for successive catalytic reduction, resulting in the growth of outer Co NPs as a shell in the AB aqueous solution, although the Au^{3+} and Co^{2+} precursors were added simultaneously. Unexpectedly, compared to the monometallic and alloy counterparts, the resultant magnetically recyclable Au@Co NPs displayed excellent catalytic activity and long-term stability towards hydrolytic dehydrogenation of aqueous AB under ambient conditions.[165] A similar approach was adopted to prepare triple layered Au/Co/Fe core–shell nanoparticles. Transmission electron microscope, energy dispersive X-ray spectroscopic, and electron energy-loss spectroscopic measurements revealed that the trimetallic Au/Co/Fe NPs have a triple-layered core–shell structure composed of an Au core, a Co-rich inter-layer, and an Fe-rich shell. The Au/Co/Fe core–shell NPs exhibit much higher catalytic activities for hydrolytic dehydrogenation of ammonia borane than the monometallic (Au, Co, Fe) or bimetallic (AuCo, AuFe, CoFe) counterparts.[165]

Very recently, we reported a facile one-step and general route for *in situ* synthesis of a series of Cu@M (M = Co, Fe, Ni) core–shell NPs under ambient conditions (Fig. 4).[166] In a typical synthesis of Cu@M (M = Co, Fe, Ni) core–shell NPs, an aqueous solution of copper(II) chloride and cobalt(II) or nickel(II) chloride or iron(II) sulfate, and polyvinylpyrrolidone K 30 (PVP) as a capping agent was introduced to a round-bottom flask containing ammonia borane. The Cu^{2+} and M^{2+} were reduced in sequence to produce core–shell structured NPs during the reduction process, in which Cu^{2+} with high reduction potentials ($Eo_{Cu(II)/Cu(I)} = +0.159$ eV *vs.* SHE; $Eo_{Cu(I)/Cu} = +0.520$ eV *vs.* SHE) was first reduced by NH_3BH_3. The generated Cu–H or/and subsequent M–H species with a strong reducing ability can further reduce M^{2+}, although it is difficult to reduce them by NH_3BH_3 due to their lower reduction potentials ($Eo_{Co(II)/Co} = -0.28$ eV *vs.* SHE; $Eo_{Fe(II)/Fe} = -0.44$ eV *vs.* SHE; $Eo_{Ni(II)/Ni} = -0.25$ eV *vs.* SHE). In this process, the preformed Cu^0 NPs, serving as *in situ* seeds/core NPs, could induce the successive growth of M^0 as a shell to thus yield Cu@M core–shell NPs. Such

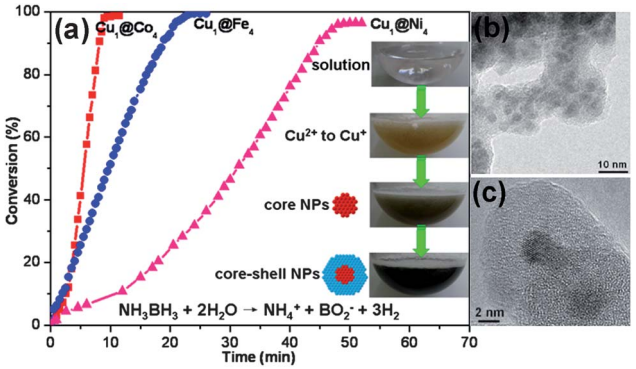

Fig. 4 (a) Hydrogen generation from NH_3BH_3 aqueous solution over Cu@Co, Cu@Fe Cu@Ni core–shell nanocatalysts under ambient conditions ($(Cu^{2+} + M^{2+})/NH_3BH_3 = 0.02$). (b) Representative TEM image of Cu@Co core–shell nanocatalyst. (c) Representative HRTEM image of Cu@Co core–shell nanocatalyst. Reprinted with permission from ref. 166. Copyright 2011 Royal Society of Chemistry.

in situ reduction and one-pot synthetic protocol for core–shell NPs is to take advantage of the differences in the reduction potentials of core and shell metal salts, where the key point is to employ a suitable reducing agent. NH_3BH_3, a moderate reducing agent, is suitable for this process. In contrast to the monometallic and alloy counterparts, the *in situ* generated bimetallic core–shell NPs have exhibited synergistic and superior catalytic activity for hydrolytic dehydrogenation of ammonia borane.

Notably, the convenience and reliability of the AB hydrolysis reaction make suitable for applications, and it has already been extensively used as a test (model) reaction for examining the catalytic activity of new nanomaterials.[148,157,166–168]

In addition to the hydrolysis of AB, methanolysis of AB has also been developed to generate hydrogen at room temperature over various catalysts [eqn (9)], such as $RuCl_3$, $RhCl_3$, $CoCl_2$, $NiCl_2$, Pd/C, RANEY® Ni, PVP-stabilized Pd NPs, zeolite stabilized Rh NPs, Co–Co_2B, Ni–Ni_3B, and Co–Ni–B, *etc.*[123,139,169,170] Hydrogen capacity from this system is about 3.9 wt%, which is lower than that from the hydrolytic system (about 7.8 wt%).

$$NH_3BH_3 + 4MeOH \rightarrow NH_4B(OMe)_4 + 3H_2 \quad (9)$$

In order to explore the liquid phase dehydrogenation of ammonia borane, a number of studies have been carried out in organic liquids and ionic liquids.[171–175] Heinekey, Goldberg and coworkers used an Ir Pincer catalyst and achieved about one equivalent of H_2 from the solution of ammonia borane in tetrahydrofuran at room temperature.[171] Baker and coworkers demonstrated that a homogeneous nickel catalyst with *N*-heterocyclic carbene (NHC) ligands releases >2.5 equiv. of H_2 gas based on ammonia borane from the solution of ammonia borane in diglyme at 60 °C.[172] Burrell and coworkers investigated dehydrogenation of AB assisted with heterogeneous Pt, Pd, Ru-catalysts in non-aqueous solution (2-methoxyethyl ether) at room temperature to 70 °C.[173] The best catalytic activity was observed for Pt. Half an equiv. of a possible three equiv. H_2 was extracted within 30 min at 70 °C, and overall close to two equiv. of H_2 was extracted from AB. Very recently, Kang and

coworkers used Pd NPs as catalyst and tetraglyme as solvent for the dehydrogenation of ammonia borane (AB) at 85 °C. Remarkably an enhanced catalytic performance was achieved to release 2.3 equiv. of H_2 in 1 h (Pd/AB = 0.019).[174] Baker, Sneddon and coworkers investigated a range of transition metal complexes as active catalysts for dehydrogenation of ammonia borane in different ionic liquids.[175] All of the complexes screened were found to give enhanced H_2 release relative to the background reaction (in the absence of catalyst under similar reaction conditions), demonstrating the viability of metal-catalyzed dehydrogenation in this ionic liquid medium. While the most active catalysts contained the precious metals Rh, Ru and Pd, the base metal precursor $Ni(COD)_2$ showed comparably high initial rates and $NiCl_2$ gave a high total H_2 release.[175] Although the hydrogen productivity from ammonia borane in organic liquid or ionic liquid is lower than hydrolysis, this process produces the BNH byproduct, which can easily be recycled (*vide infra*).

Recently, two methods involving water but no catalysts have been developed for releasing hydrogen from AB.[176–178] One is based on combustion of AB mixtures with aluminum powder and gelled water. It was experimentally shown that these mixtures, upon ignition, exhibit self-sustained combustion with hydrogen release from both AB and water, 7.7 wt% H_2 in total. The other method involves external heating of aqueous AB solutions to ~120 °C or higher under argon pressure to avoid water boiling. Experiments show that heating aqueous AB solutions to temperatures 117–170 °C releases 3 equiv. of hydrogen per mole AB, where 2.0–2.1 equiv. originate from AB and 0.9–1.0 equiv. from water.

In order to search for new BN-based liquid-phase hydrogen storage materials, recently, Liu and coworkers developed BN-methylcyclopentane (**1**), which is an air- and moisture-stable liquid at room temperature.[179] It is capable of releasing 2 equiv. of H_2 per molecule (4.7 wt%) both thermally, at temperatures above 150 °C, and catalytically, using a variety of cheap and abundant metal halides at temperatures below 80 °C (Fig. 5). The exclusive product of dehydrogenation is the trimer (**2**), which is also a liquid at room temperature. They also demonstrated that the conversion of the spent fuel (**2**) back to the charged fuel (**1**) can be accomplished in high yield, making this system a viable candidate for liquid-phase hydrogen storage in mobile applications.

3.2 Regeneration of ammonia borane

The hydrolysis and dehydrogenation processes can effectively release hydrogen from ammonia borane under mild conditions. However, the viability of any chemical hydrogen storage system is critically dependent on efficient recyclability, but reports on the latter subject are sparse.[21,123,180–184] The ^{11}B NMR spectroscopy analyses of spent fuels indicated that the byproducts in the hydrolysis of AB are mainly borate species.[16,87,135,185–188] Generally speaking, a significant drawback of solvolysis, as in the case of $NaBH_4$, is that B–H bonds are converted to much stronger B–O bonds, resulting in a more exothermic reaction than dehydrogenation. Therefore, regeneration of spent fuel requires strong reducing agents.

It has been reported that ammonia borane can be synthesized in high yield by the combination of sodium borohydride and ammonium sulfate ($(NH_4)_2SO_4$) or ammonium chloride (NH_4Cl) (eqn (10)).[123,180]

$$2NaBH_4 + (NH_4)_2SO_4 \xrightarrow{THF,40^\circ C} 2NH_3BH_3 + Na_2SO_4 + 2H_2 \quad (10)$$

Further, it has also been reported that hydrolysis of sodium borohydride and ammonia borane both generate borates as spent fuel.[189] Therefore, the processes developed to recycle the spent fuel of sodium borohydride (Section 2.2) could be used for recycling the spent fuel of ammonia borane. Chen and coworkers suggested a total life cycle of hydrogen release and regeneration of NH_3BH_3 and $NaBH_4$ (Fig. 6).[190] In brief, since boric acid is the main hydrolysis product of ammonia borane hydrolysis, it is possible at first to produce trimethyl borate, $B(OCH_3)_3$, from esterification of boric acid with methanol.[95,191] The Brown–Schlesinger process[192] would further convert as-obtained trimethyl borate to sodium borohydride by reacting it with sodium hydride (NaH). Lastly, ammonia borane is synthesized from sodium borohydride reacting with ammonia sulfate in tetrahydrofuran (THF) at 40 °C.[123]

Ramachandran and Gagare demonstrated a system based on transition metal catalyzed solvolysis of AB to yield $[NH_4][B(OMe)_4]$ [eqn (9)], which could be converted back to AB by treatment with NH_4Cl and lithium aluminium hydride [eqn (11)].[123] It is likely to be energetically costly to convert the oxidation product, $Al(OMe)_3$, back to the complex hydride.

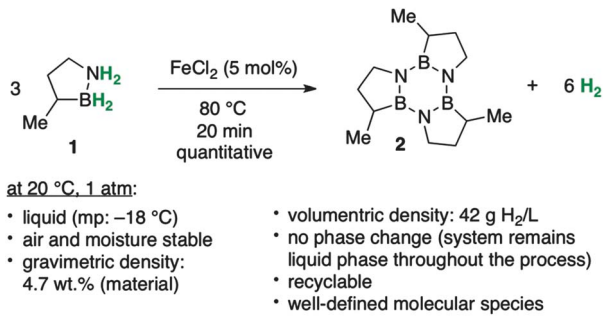

Fig. 5 A single-component liquid-phase hydrogen storage material. Reprinted with permission from ref. 179. Copyright 2011 American Chemical Society.

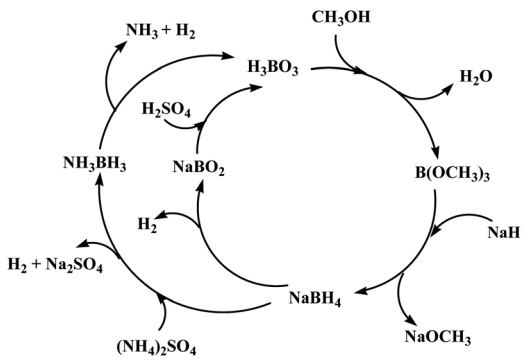

Fig. 6 Proposed total life cycle of ammonia borane and sodium borohydride for hydrogen generation and regeneration. Reprinted with permission from ref. 190. Copyright 2011 Elsevier.

$$NH_4B(OMe)_4 + LiA1H_4 + NH_4Cl \xrightarrow{THF,8h,rt,sealed\ container} NH_3BH_3 + Al(OMe)_3 + MeOH + H_2 + LiCl + NH_3 \quad (11)$$

Studies have been revealed that the spent fuels obtained after dehydrogenation of ammonia borane are generally BNH materials. The composition of spent fuel depends on the dehydrogenation method.[21,22] A homogeneous nickel catalyst with N-heterocyclic carbene (NHC) ligands, developed by Baker and coworkers, is capable of greater release than two equivalents of H_2 from the solution of ammonia borane in diglyme at 60 °C and gives polyborazylene (PB), which is a BNH material (containing a B–N linkage), as a single spent fuel component.[172] The strategies presented to date for regeneration of BNH-spent fuel involve two important steps, digestion and reduction. Addition of an acid (HX) can protonate these linkages, releasing amine and making B–X bonds (digestion). The B–X bonds can then be reduced by chemical reductants to form B–H bonds.[181,193,194] Sutton, Gordon, Power and coworkers described an energy efficient regeneration process for polyborazylene (PB) spent fuel.[182] In this scheme, effective digestion of polyborazylene with 1,2-benzenedithiol was demonstrated to form ammonia adducts of dithioboron compounds. These compounds contain relatively weak B–S bonds that are readily reduced by Sn–H. Very recently, this group demonstrated that the spent fuel derived from the removal of greater than two equivalents of H_2 per molecule of AB (*i.e.*, polyborazylene, PB) can be converted back to AB nearly quantitatively by treatment with hydrazine (N_2H_4) in liquid ammonia (NH_3) at 40 °C in a sealed pressure vessel (Scheme 1).[184] For practical application this regeneration process of ammonia borane must be as energetically efficient as possible, so no reaction step can be too exo- or endothermic.

3.3 Conclusions

The 19.6 wt% H_2 in AB has made it an attractive molecule for chemical hydrogen storage. Besides dehydrogenation of AB, hydrolysis of AB presents a high hydrogen capacity up to 7.8 wt % of the starting materials. In comparison with $NaBH_4$, which undergoes self-hydrolysis in water without catalysts, AB has the advantage that it is stable in aqueous solution, which makes AB a promising hydrogen storage system. A portable hydrogen generation system is expected to be established on the basis of the metal-catalyzed dissociation and hydrolysis of AB. The AB hydrolysis reaction proceeds under ambient conditions with rapid kinetics in the presence of suitable catalysts; not only noble metal but also many highly active non-noble metal-based catalysts have been developed. For practical applications of AB hydrolytic dehydrogenation in portable electric devices, further experimental and theoretical studies for pending limitations, such as (i) how to break the strong B–O bonds formed during the H_2 generation to recycle the end products and (ii) how to reduce the catalyst deactivation, *etc.*, are highly desired to overcome the high material cost issue.

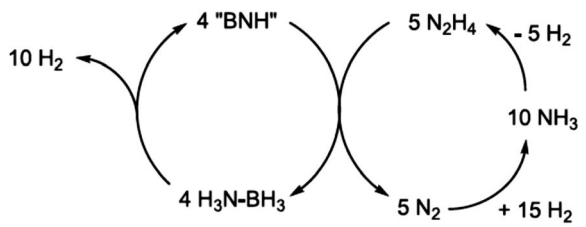

Scheme 1 Ideal overall reaction scheme for AB (NH_3BH_3) regeneration from PB ("BNH") with hydrazine (N_2H_4). Reprinted with permission from ref. 184. Copyright 2011. The American Association for the Advancement of Science.

4. Hydrazine

4.1 Catalytic decomposition of hydrous hydrazine

Anhydrous hydrazine (H_2NNH_2, HZ), a liquid at room temperature, has a hydrogen content as high as 12.5 wt%. It is a colorless oily liquid at room temperature and used as a monopropellant in satellite propulsion.[195,196] This compound is hypergolic; it explosively reacts upon exposure to a metal surface. Studies, mostly on the reactions of hydrazine highly diluted in inert gases such as argon, have shown that hydrazine can be decomposed on supported metals,[197] metal nitrides,[198,199] or metal carbides[200,201] in two ways: incomplete decomposition [eqn (12)],

$$3H_2NNH_2 \rightarrow 4NH_3 + N_2(g) \quad (12)$$

and the complete decomposition [eqn (13)]:

$$H_2NNH_2 \rightarrow N_2(g) + 2H_2(g) \quad (13)$$

The decomposition pathway depends on the catalyst used and also on applied reaction condtions.[197,199,201–206] Most of the reported catalysts show a high activity for reaction [eqn (12)] at temperatures below 300 °C.[197,199–206] Hydrogen generation from hydrazine over these catalysts was observed at high temperature due to the decomposition of NH_3. Interestingly, the SiO_2-supported Ni, Pd, and Pt catalysts were active even at around room temperature and the Ni/SiO_2 catalyst shows 90% selectivity for hydrogen at 50 °C.[197] The hydrogen selectivity increases with the reaction temperature in the range of 30–80 °C, and then quickly decreases when the reaction temperature is further increased. It is suggested that two competing reactions (12) and (13) are occurring during hydrazine decomposition over these supported catalysts. At higher temperature (>400 °C), the hydrogen selectivity tends to increase again (~100%) due to the decomposition of NH_3.

The explosive nature of anhydrous hydrazine (>98%) upon exposure to metal catalysts surface limits its application from safety point of view. Hydrous hydrazine, such as hydrazine monohydrate, $H_2NNH_2 \cdot H_2O$, still contains a large amount of hydrogen, 8.0 wt%, which is available for hydrogen generation and is much safer,[196] while efforts need to be made from the engineering side to minimize the influence of toxicity. Notably, generation of only nitrogen as byproduct in addition to hydrogen, which does not need on-board collection for recycling, and easy recharging using the current infrastructure of liquid fuels are distinct advantages of hydrous hydrazine. These advantages of hydrous hydrazine make it a promising hydrogen carrier for storage and transportation. The key to exploit effectively the hydrogen-storage properties of hydrazine is to develop

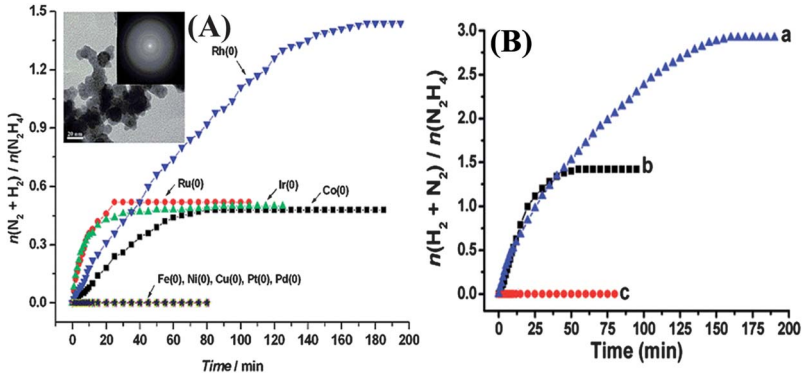

Fig. 7 (A) Time-course plots for the decomposition of hydrazine in aqueous solutions in the presence of different metal NPs (metal/N_2H_4 = 1 : 10) at 298 K. The inset shows a TEM image of Rh(0) NPs and the corresponding SAED pattern. (B) Time course plots for decomposition of hydrous hydrazine (0.5 M) catalyzed by (a) Rh_4Ni, (b) Rh, and (c) Ni nanocatalysts (M/N_2H_4 = 1 : 10) at 25 °C. Reprinted with permission from ref. 26 and 27. Copyright 2011 American Chemical Society.

efficient and selective catalysts for H_2 generation from hydrous hydrazine.[26,27,207–214] It has been reported that an Ir/Al_2O_3 catalyst is active for hydrazine monohydrate decomposition, while no quantitative results were reported in this work.[207] In the beginning of our study toward catalytic decomposition of hydrous hydrazine, we investigated the catalytic activity of various metal (Fe, Co, Ni, Cu, Ru, Rh, Ir, Pt and Pd) nanoparticles at room temperature (Fig. 7A and Table 3).[26] Among the various NPs examined, the Rh NPs were found to be the most selective (~44%) for hydrogen release from hydrous hydrazine decomposition. Other metal NPs, such as Co, Ru and Ir, exhibited only 7% selectivity for hydrogen, and Fe, Cu, Ni, Pt and Pd are totally inactive under the described reaction condition.[26]

Bimetallic NPs generally show composition-dependent surface structures and therefore potential for improving catalytic performances.[215,216] Usually, co-reduction with a relatively strong reducing agent can be used for the preparation of bimetallic alloy NPs. We also adopted this method and investigated the catalytic activities of a series of bimetallic alloy NPs towards catalytic decomposition of hydrous hydrazine. We investigated the catalytic activities of Rh_xNi_y (Rh/Ni = 1 : 16–64 : 1) nanocatalysts to hydrous hydrazine decomposition reaction with the Rh/N_2H_4 molar ratio (1 : 10) kept unchanged and found that the selectivity to hydrogen strongly depends on the Rh/Ni ratio.[27] Surprisingly, despite Ni NPs being inactive and the low H_2 selectivity of Rh NPs to this reaction, the alloying of Ni and Rh drastically enhances the hydrogen selectivity. The H_2 selectivity was found to be strongly dependent on the Rh–Ni ratio, and a maximum of H_2 selectivity at 100% was reached at Rh–Ni = 4 : 1 (Fig. 7B and Table 3).[27] Moreover, alloying Rh with other first-row transition metals, such as Fe, Co, and Cu, exhibits a loss in hydrogen selectivity, under the analogous synthetic and reaction conditions.[27] Generally speaking, alloy materials have distinct binding properties with reactants, in contrast to those for monometallic metal catalysts. It is reasonable to assert that the alloying of Rh and Ni leads to a modification of the catalyst surface and tunes the interactions of Rh with the N–N and N–H bonds as well as the stability of reaction intermediates on the catalyst surface.[201,206] Consequently, the reaction prefers pathway (13) to pathway (12), resulting in a complete conversion of hydrazine to hydrogen and nitrogen.

Table 3 Catalytic activities of metal catalysts for decomposition of hydrous hydrazine

Catalysts	Temp. (°C)	H_2-selectivity (%)	Ref.
Ni	25	0	26
	50	33	211
Co	25	7	26
Fe	25	0	26
Cu	25	0	26
Ru	25	7	26
Rh	25	43.8	26
Pd	25	0	26
Ir	25	7	26
Pt	25	0	26
Rh_4Ni	25	100	27
Ni–Pt	25	100	208
Ni–Ir	25	100	209
Ni–Pd	50	80	210
Ni–Fe	25	0	212
	70	100	212
Rh–Ni/graphene	25	100	213
Ni–Al hydrotalcite	30	93	214

In another report, we demonstrated that the alloying of nickel and platinum makes it possible to achieve 100% selectivity for the decomposition of hydrazine in aqueous solution to hydrogen at room temperature, whereas the monometallic nickel and platinum counterparts are inactive for this reaction.[208] The bimetallic Ni–Pt nanocatalyst with the platinum content as low as 7 mol% ($Ni_{0.93}Pt_{0.07}$) presents a step toward a high-performance catalyst system.[208] In order to search for new catalysts, we found a surfactant-stabilized highly active bimetallic $Ni_{0.95}Ir_{0.05}$ alloy nanocatalyst prepared by alloying Ir (5 mol%) with Ni (95 mol%), which exhibits 100% H_2 selectivity for complete decomposition of hydrous hydrazine at room temperature.[209] Notably, the corresponding monometallic counterpart has poor H_2 selectivity (7% H_2 selectivity, Ir NPs) or is inactive (Ni NPs).

Further, we reported Ni–Pd bimetallic nanoparticle catalysts ($Ni_{1-x}Pd_x$), synthesized by alloying Ni and Pd with varying Pd contents, which exhibit appreciably high H_2 selectivity (>80% at $x = 0.40$) from the decomposition of hydrous hydrazine at 50 °C, whereas the corresponding monometallic counterparts are either

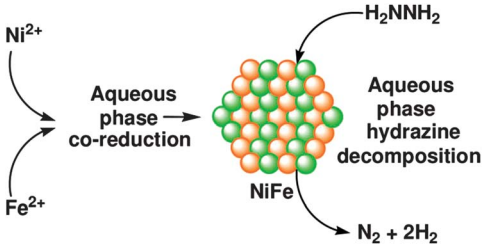

Scheme 2 NiFe nanocatalyst preparation and hydrazine decomposition. Reprinted with permission from ref. 212. Copyright 2011 American Chemical Society.

inactive (Pd NPs) or poorly active (Ni NPs exhibit 33% H_2 selectivity).[210] Unlike the high activity of Ni–Pd nanocatalysts, Pd–M (M = Fe, Co and Cu) bimetallic nanocatalysts exhibit poor catalytic activity.

A high-performance catalyst system with low noble metal content might facilitate the application of hydrous hydrazine as a highly promising practical material for hydrogen storage. Therefore, emphasis has been placed on the development of suitable reaction conditions for hydrazine decomposition to hydrogen by using low-cost nanocatalysts. We have observed that Ni NPs, which are inactive for the decomposition of hydrous hydrazine at room temperature, can show drastically enhanced catalytic activity with an H_2 selectivity of 33% when the reaction temperature is raised to 50 °C (Table 3).[211] This significant temperature effect can be suitably exploited to achieve 100% H_2 selectivity at 50 °C by alloying Ni and Pt with a Pt content as low as 1 mol%. These results indicate that a suitable reaction temperature may make it possible to achieve high catalytic performance for hydrogen generation by decomposition of hydrous hydrazine with Ni-based nanocatalysts with low content of noble metals.[211]

After having the high catalytic performance of the Ni and noble metal (Rh, Pt, Ir) based bimetallic nanoparticle catalysts (nanocatalysts), we extended our studies toward the development of a completely noble-metal-free catalyst, which is crucial for promoting the potential application of hydrous hydrazine as a hydrogen storage material. In this regard, we found high-performance noble-metal-free bimetallic Ni–Fe NP catalysts for selective decomposition of hydrous hydrazine to hydrogen under moderate conditions.[212] Bimetallic Ni–Fe nanocatalysts were prepared using a surfactant-aided coreduction process (Scheme 2). To an aqueous solution of nickel(II) chloride and ferrous(II) sulfate was added an aqueous solution of sodium borohydride in the presence of hexadecyltrimethylammonium bromide (CTAB) (Scheme 2).[212] Ni_3Fe, NiFe, and $NiFe_3$ represent the Ni–Fe nanocatalysts prepared with varying compositions of Ni and Fe, with Ni–Fe molar ratios of 3 : 1, 1 : 1 and 1 : 3, respectively.

Investigations of the catalytic performance of Ni–Fe nanocatalysts with various Ni–Fe molar ratios for the decomposition of hydrous hydrazine at 70 °C suggested a significant dependence of the hydrogen selectivity on the composition of the nanocatalyst (Fig. 8). Although the NiFe nanocatalyst exhibited the highest catalytic performance among the examined Ni–Fe nanocatalysts, only 81% hydrogen selectivity was achieved.[212] Surprisingly, it was found that the addition of NaOH significantly enhanced the H_2 selectivity. The NiFe nanocatalyst released gases in a stoichiometric amount (3.0 equiv.) from the decomposition of hydrous hydrazine in 190 min (catalyst/H_2NNH_2 = 1 : 10) with NaOH (0.5 M) at 70 °C (Fig. 8), corresponding to decomposition of hydrous hydrazine to hydrogen with 100% selectivity *via* pathway (13).[212] In addition, the NiFe catalyst exhibited high stability. The possible reason for the effects of the alkaline additive might be understood as follows: pathway (12) gives the basic product NH_3; the addition of NaOH may make the catalyst surface highly basic, which may be unfavorable for the formation of basic NH_3 and therefore for pathway (12). In contrast to the NiFe nanocatalyst, 89% hydrogen selectivity was observed for the Ni_3Fe nanocatalyst, whereas the $NiFe_3$ nanocatalyst exhibited 71% hydrogen selectivity for the decomposition of hydrous hydrazine at 70 °C (Fig. 8A). Notably, addition of weaker bases (*e.g.*, NH_3, CH_3COONa) had no effect on the catalytic performance of the NiFe catalysts. Improvements in the catalytic performance due to addition of NaOH were also observed for $Ni_{45}Pt_{55}$ and $Ni_{50}Ir_{50}$ catalysts; the addition of NaOH (0.5 M) resulted in increases in the H_2 selectivity from 61 to 86% for $Ni_{45}Pt_{55}$ and 7 to 95% for $Ni_{50}Ir_{50}$ at 25 °C, indicating that the presence of alkaline additives is commonly beneficial in promoting pathway (13).[212]

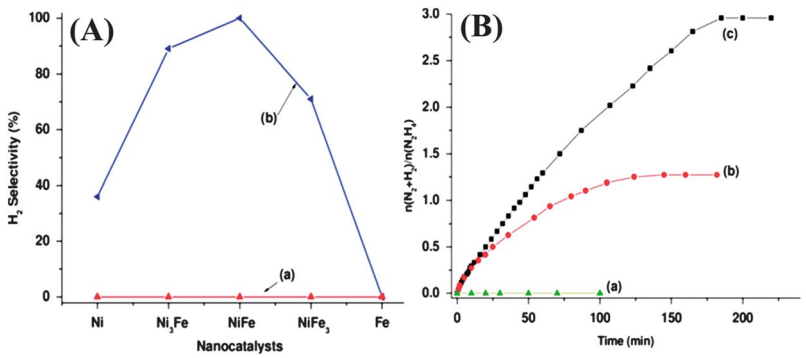

Fig. 8 (A) Comparison of H_2 selectivities in the decomposition of hydrous hydrazine (0.5 M) to hydrogen in the presence of Ni, Ni_3Fe, NiFe, $NiFe_3$, and Fe nanocatalysts (catalyst/H_2NNH_2 = 1 : 10) with NaOH (0.5 M) at (a) 25 and (b) 70 °C. (B) Time-course plots for the decomposition of hydrous hydrazine (0.5 M) to hydrogen in the presence of (a) Fe, (b) Ni, and (c) NiFe nanocatalysts (catalyst/H_2NNH_2 = 1 : 10) with NaOH (0.5 M) at 70 °C. Reprinted with permission from ref. 212. Copyright 2011 American Chemical Society.

None of the Ni–Fe NPs catalysts was found to be active for this reaction when examined at 25 °C with or without NaOH, indicating the crucial role of temperature in the decomposition reaction (Fig. 8A). Fe NPs prepared under analogous conditions exhibit no activity for this reaction at 25 °C or at elevated temperatures (thermal decomposition of hydrazine in absence of catalyst is ~250 °C).[196] Ni NPs, which are also inactive at room temperature for the decomposition of hydrous hydrazine, can show an enhancement in the activity with an increase in the reaction temperature.[211,212] An investigation of the role of temperature on the NiFe nanocatalyst showed enhanced activity and H_2 selectivity for decomposition of hydrazine to hydrogen at elevated temperatures. Although the NiFe catalyst was inactive at 25 °C, the activity was enhanced along with the enhancement in H_2 selectivity to 80% at 50 °C and 100% at 70 °C in the presence of NaOH (0.5 M).

Recently, Zhang and coworkers prepared graphene-supported RhNi catalyst by a facile co-reduction route, wherein the graphene plays a key role as a dispersion agent and distinct support for the RhNi NPs.[213] The RhNi catalyst prepared in the presence of GO and NaOH exhibits 100% H_2 selectivity [$n(N_2 + H_2)/nN_2H_4 = 3.0$] and high activity to complete the decomposition reaction of hydrous hydrazine within only 49 min (Rh/N_2H_4 = 1/10) at room temperature, which is faster (as high as 327%) than that of the most active catalysts previously reported for this reaction.[26,27,208,209]

Very recently, Zhang and coworkers found that the hydrotalcite supported Ni catalyst (78 wt% Ni–Al_2O_3–HT) exhibits 100% conversion and 93% H_2 selectivity for the decomposition of hydrous hydrazine. In the presence of 78 wt% Ni–Al_2O_3–HT (50 mg) catalyst, the reaction can be completed in 13 min ($Ni/N_2H_4 = 1:2.4$) at 50 °C and in 70 min at 30 °C.[214] This unique catalysis is due to the cooperation of Ni NPs and the strong basic sites of the hydrotalcite host.

4.2 Synthesis of hydrazine

Decomposition of hydrazine generates nitrogen gas as a byproduct in addition to hydrogen (H_2). The recycling of nitrogen (N_2) to hydrazine is very crucial for the development of hydrazine-based hydrogen storage cycling. There are several methods reported in the literature for synthesis of hydrazine, but most of the synthetic processes involve different nitrogen containing materials other than nitrogen gas.[196,217] The commercial-scale production of hydrazine is based on the Raschig process [eqn (14)–(16)], the Schestakov synthesis [eqn (17)], the Bayer process [eqn (18) and (19)], and the H_2O_2 process [eqn (20) and (21)] *etc.*[196,217] These processes mainly involve NH_3 or urea as the starting material.

Raschig process:

$$2NaOH + Cl_2 \rightarrow NaOCl + NaCl + H_2O \quad (14)$$

$$NaOCl + NH_3 \rightarrow NH_2Cl + NaOH \quad (15)$$

$$2NH_3 + NH_2Cl \rightarrow N_2H_4 + NH_4Cl \quad (16)$$

Schestakov synthesis:

$$(H_2N)_2C{=}O + NaOCl + 2NaOH \rightarrow N_2H_4 + H_2O + NaCl + Na_2CO_3 \quad (17)$$

Bayer process:

$$NaOCl + 2NH_3 + 2CH_3COCH_3 \rightarrow (CH_3)_2C{=}N{-}N{=}C(CH_3)_2 + NaCl + 3H_2O \quad (18)$$

$$(CH_3)_2C{=}N{-}N{=}C(CH_3)_2 + 2H_2O \rightarrow 2CH_3COCH_3 + N_2H_4 \quad (19)$$

H_2O_2 process:

$$H_2O_2 + 2NH_3 + 2C_2H_5COCH_3 \rightarrow (C_2H_5)(CH_3)C{=}N{-}N{=}C(CH_3)(C_2H_5) + 4H_2O \quad (20)$$

$$(C_2H_5)(CH_3)C{=}N{-}N{=}C(CH_3)(C_2H_5) + 2H_2O \rightarrow 2C_2H_5COCH_3 + N_2H_4 \quad (21)$$

The search for selective reduction of nitrogen has not yet found a practical or economic solution. Ammonia remains a valuable nitrogen-containing starting material for the production of hydrazine.[196,217,218] The approach from nitrogen and hydrogen to hydrazine might be the transformation of nitrogen to ammonia (the Haber–Bosch process, homogeneous catalytic processes, or an electrolytic process) and then to hydrazine on a large scale [eqn (22)] or perhaps, preferably, transformed directly to hydrazine by means of an electrolytic process similar to that for ammonia synthesis.[217–223]

$$N_2 + 3H_2 \rightarrow 2NH_3 \rightarrow N_2H_4 + H_2 \quad (22)$$

4.3 Conclusions

Hydrazine seems to be a promising hydrogen storage system due to its uncomplicated byproduct and easy storage. For the decomposition, many efficient catalysts have been developed and studied in detail. Further developments of low-cost, high-performance catalysts are needed for the practical use of hydrous hydrazine as an effective hydrogen storage material. The effective practical application of hydrazine will be economically feasible if low-cost production of hydrazine can be achieved by finding an effective method of conversion of nitrogen to hydrazine.

5. Hydrazine borane

5.1 Catalytic hydrogen generation from aqueous hydrazine borane

Hydrazine borane ($N_2H_4BH_3$, HB) has a gravimetric hydrogen storage capacity of 15.4 wt%.[117] Like AB, the aqueous solution of HB (solubility of 6 g per 100 g H_2O at 25 °C)[224,225] is quite stable against spontaneous hydrolysis; for instance, over 3 weeks of storage under inert atmosphere at room temperature. Hydrazine borane can release hydrogen through chemical pathways such as thermolysis or hydrolysis.[226] HB starts to decompose slowly at around 60 °C. Better dehydrogenation kinetics and extents are achieved at elevated temperatures, higher than 100 °C. The release of hydrogen from HB in the presence of LiH has been reported upon heating at a temperature range of 100–150 °C (for example, 4.4 equiv. H_2 per HB + LiH at 100 °C upon 45 h heating).[227] Its dehydrogenation by catalytic hydrolysis has been also reported by Özkar and coworkers.[224] They reported that the

hydrogen generation can readily be achieved from the hydrolysis of hydrazine borane by using $RhCl_3$ precatalyst, in which bulk Rh(0) was found to be an active catalyst providing a TOF value of 12 000 h^{-1} even at room temperature. They used rhodium(0) nanoparticles supported on hydroxyapatite ($Ca_{10}(OH)_2(PO_4)_6$, HAP) as catalyst and observed a TOF value of 6700 h^{-1}.[228] However, only 3/7 of its hydrogen was recovered by hydrolysis of the BH_3 group and the hydrazine group was not decomposed [eqn (23)].[224,228] Karahan *et al.* reported the metal catalyzed methanolysis of hydrazine borane using a nickel(II) chloride precatalyst at room temperature.[229] The methanolic solution of HB (HB/Ni $\geq$ 200) can release 3 equiv. of H_2, corresponding to methanolysis of the BH_3 unit, with a rate of 24 mol H_2 (mol Ni min)$^{-1}$ at room temperature.[229]

$$N_2H_4BH_3 + 3H_2O \rightarrow N_2H_4 + B(OH)_3 + 3H_2 \quad (23)$$

Hydrolysis of BH_3 unit of HB leads to occurrence of free N_2H_4.[224,228] It is therefore reasonable to consider that the presence of a selective catalyst is crucial to achieve the complete HB dehydrogenation. Unlike the NH_3 group of AB, the N_2H_4 group of HB can also be dehydrogenated in the presence of a selective catalyst [eqn (24)], although this reaction is in competition with NH_3 release [eqn (25)].

$$\alpha N_2H_4 \rightarrow \alpha N_2 + 2\alpha H_2 \quad (24)$$

$$(1 - \alpha)N_2H_4 \rightarrow 4(1 - \alpha)/3NH_3 + (1 - \alpha)/3N_2 \quad (25)$$

$$N_2H_4BH_3 + 3H_2O \rightarrow B(OH)_3 + (3 + 2\alpha)H_2 + (2\alpha + 1)/3N_2 + 4(1 - \alpha)/3NH_3 \quad (26)$$

Being inspired by studies on hydrous hydrazine decomposition,[27,208,209] bimetallic metallic nanocatalysts that are active for decomposition of hydrous hydrazine, which are also active for hydrolysis of $-BH_3$ group, have been used for complete dehydrogenation of HB in aqueous solution.[24] Use of a Pt nanocatalyst at 50 °C only permits release of *ca.* 2.98 $\pm$ 0.05 equiv. H_2 per HB, which originates from hydrolysis of the BH_3 group [eqn (23)]. On the other hand, in the presence of the Ni nanocatalyst, some H_2 and N_2 from the N_2H_4 group evolve, which corresponds to 3.22 $\pm$ 0.05 equiv. $H_2 + N_2$ (Fig. 9). The presence of a small amount of Pt in a Ni–Pt NP has a significant beneficial effect on N_2H_4 decomposition (Fig. 9). $Ni_{0.97}$–$Pt_{0.03}$ releases 5.07 $\pm$ 0.5 equiv. $H_2 + N_2$ per HB. By increasing the Pt content up to 0.11 mol% ($Ni_{0.89}$–$Pt_{0.11}$), there is an increase up to 5.79 $\pm$ 0.05 equiv. $H_2 + N_2$ per HB whereas the hydrogen selectivity reaches the value 93 $\pm$ 1% [eqn (26)]. A further increase of the Pt content (0.17 and 0.23 mol%) has a detrimental effect since the H_2 mol number slightly decreases to 5.29 $\pm$ 0.05 equiv. $H_2 + N_2$ per HB. In fact, the variation of the mol number of [$H_2 + N_2$] as a function of the Pt content has a volcano shape (Fig. 9b), and the maximum peak is observed for Pt = 0.11 mol% ($Ni_{0.89}Pt_{0.11}$). Electronic and/or geometric effects could rationalize such reactivity changes.[230,231] It can be seen that the observed kinetics of the dehydrogenation of the N_2H_4 group is similar to that of the decomposition of neat hydrazine with the same NiPt catalysts.[208]

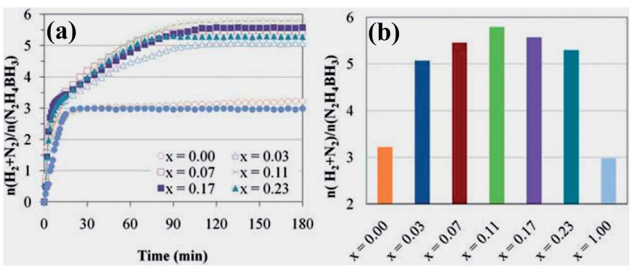

Fig. 9 (a) Time course profiles and (b) Pt-content dependence of $n(H_2 + N_2)/n(N_2H_4BH_3)$ for dehydrogenation of $N_2H_4BH_3$ in the presence of the $Ni_{1-x}Pt_x$ nanocatalysts at 50 °C. Reprinted with permission from ref. 24. Copyright 2011 Royal Society of Chemistry.

Very recently, a series of Ni-based bimetallic systems have been investigated with Pt, Ru, Rh or Ir as the second metal.[232] The results show that most of the $Ni_{1-x}M_x$ nanocatalysts outperform the monometallic Ni, Pt, Ru, Rh and Ir catalysts. The best performance achieved is 5.1 $\pm$ 0.05 mol ($N_2 + H_2$) per mol(HB) with $Ni_{0.89}Rh_{0.11}$ and $Ni_{0.89}Ir_{0.11}$, suggesting the occurrence of the following reaction [eqn (27)]:

$$N_2H_4BH_3 + 3H_2O \rightarrow B(OH)_3 + 4.3H_2 + 0.8N_2 + 0.6NH_3 \quad (27)$$

5.2 Synthesis of hydrazine borane

Several attempts by Goubeau and Ricker using various reagents (B_2H_6, $LiBH_4$, $NaBH_4$, N_2H_4, and $(N_2H_5)_2SO_4$) showed that the most efficient HB synthesis process involved $NaBH_4$ and $(N_2H_5)_2SO_4$ in dioxane [eqn (28)].[233]

$$2NaBH_4 + (N_2H_5)_2SO_4 \rightarrow 2N_2H_4BH_3 + 2H_2 + Na_2SO_4 \quad (28)$$

Recently, Demirci and coworkers reported a modified procedure of this synthetic method by using a 2-step synthesis (salt metathesis and solvent extraction–drying) through which $N_2H_4BH_3$ is successfully obtained in 3 days, with a yield of about 80% and a purity of 99.6%.[226] In addition, several alternative processes for preparing HB have also been reported,[234–236] which typically consisted of a BH_3 source, mainly $NaBH_4$, and a N_2H_4 source, either $N_2H_4 \cdot HCl$ or $MgCl_2 \cdot 4N_2H_4$, in an organic solvent (benzene, dioxane, hexane, THF) under ambient condition (yields 33–98%). Another approach was to use directly N_2H_4 as solvent at 0 °C. For a 2 days process, the yield was low (34%) with a purity of 98% whereas for a longer time (1 week) yields up to 79% were achieved.

Like sodium borohydride and ammonia borane, hydrazine borane also produces borates as byproducts in the dehydrogenation reaction in water. Therefore, the processes developed to recycle the spent fuel of sodium borohydride (Section 2.2) could be used for recycling the spent fuel of hydrazine borane. The as-sythesized sodium borohydride upon reaction with $(N_2H_5)_2SO_4$ can generate hydrazine borane. More recently, Sutton, Gordon and coworkers interestingly obtained HB as a major product (70–100%) while they were working on reacting spent fuel polyborazylene (PB) with N_2H_4 (12 h) to obtain AB.[184,237] Future study in this direction could be to find a low cost and efficient regeneration of hydrazine borane from the byproduct obtained after hydrogen release.

5.3 Conclusions

Hydrazine borane is emerging as one of the most promising solid hydrogen carriers due to its high gravimetric hydrogen storage capacity (15.4 wt%). The current catalyst systems are able to generate hydrogen from hydrolysis of the BH_3 part, or both hydrolysis of BH_3 and decomposition of the hydrazine part. However, like sodium borohydride and AB, HB will certainly face issues related to the use of water in excess (because of low solubility and of hydration of spent fuel, borate by-products), catalyst durability, by-products recyclability, and cost. Sodium borohydride, AB and HB should then be judged as equal for these specific problems. Nevertheless, the present challenges are now to find a more selective catalyst enabling one to reach 100% selectivity to hydrogen – the catalyst activity should be also stable – and to better understand the fundamentals of the reactions occurring.

6. Formic acid

6.1 Catalytic decomposition of formic acid

Formic acid, the simplest carboxylic acid, is a non-toxic liquid (although neat formic acid is corrosive and its vapour is harmful) at room temperature with a density of 1.22 g cm^{-3}, which is suitable for easy transportation, refueling, and handling.[28] Formic acid and its conjugated base, formate, have been used widely as a hydrogen source in transfer hydrogenation reactions.[238,239] Formic acid has a hydrogen content of 43 g kg^{-1}, corresponding to 4.4 wt% hydrogen, and produces only gaseous products (H_2–CO_2) by decomposition. The H_2–CO_2 mixture can be easily separated under certain conditions.[28]

$$HCOOH \rightarrow H_2 + CO_2 \; \Delta G = -48.4 \text{ kJ mol}^{-1} \quad (29)$$

$$HCOOH \rightarrow H_2O + CO \; \Delta G = -28.5 \text{ kJ mol}^{-1} \quad (30)$$

The decomposition of formic acid follows two principal pathways, in which the process producing CO_2 and H_2 [eqn (29)] is the desired reaction and that producing CO and H_2O [eqn (30)] is the undesired side reaction.[240] The selective decomposition of formic acid to CO_2 and H_2, which is the reversible reaction of CO_2 hydrogenation, is crucial for formic acid based hydrogen storage.[241] The combination of carbon dioxide and formic acid as a hydrogen storage system might act as an elegant and simple concept wherein selective decomposition of formic acid to H_2 and CO_2 and recycling of CO_2 by H_2 reduction to formic acid can be achieved (Scheme 3).[242,243] Meanwhile, CO_2 is abundant on the Earth; it is cheap, and readily available. In this case, a reduction of CO_2 emissions is the use of CO_2 itself as a hydrogen carrier.

6.1.1 Homogeneous catalytic decomposition of formic acid. Homogeneous catalysts are widely used for the decomposition of formic acid. A pioneering study in homogenous catalysis was done by Coffey in 1967.[244] This report described the use of soluble metal complexes for selective decomposition of formic acid to carbon dioxide rather than carbon monoxide. A series of Pt, Ru and Ir phosphine complexes have been tested, among which $IrH_2Cl(PPh_3)_3$ gave the highest rate of decomposition. Another report described the $Rh(C_6H_4PPh_2)(PPh_3)_2$

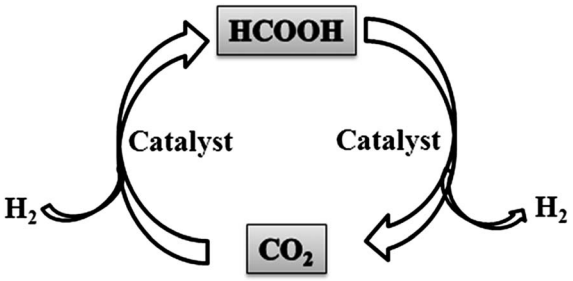

Scheme 3 The hydrogen storage system based on carbon dioxide–formic acid (CO_2–HCOOH).

organometallic complex as an active catalyst for the decomposition of formic acid.[245] In 1982 Paonessa and Trogler found that a platinum dihydride complex catalyzed the reversible formation of carbon dioxide and hydrogen from formic acid in a process that was somewhat dependent on the choice of solvent, and promoted by the addition of a small amount of sodium formate.[246] King and Battacharyya found rhodium(III) catalyzed formic acid decomposition to hydrogen in aqueous solution and nitrate ions were capable of promoting this reaction.[247] A molybdenum hydride complex for formic acid decomposition has been reported; the use of the hydride was important, as the equivalent halide complexes were inactive in this application.[248] Detailed mechanism studies of formic acid decomposition process and X-ray crystallographic characterization of the intermediates were carried out by Puddephatt and coworkers using a binuclear, diphosphine-bridged, diruthenium catalyst.[249,250] This catalyst was the most active catalyst for this reaction at that time. The reversibility of the reaction was also studied, and the same catalyst was found to be competent in the formation of formic acid by hydrogenation of carbon dioxide. Performances of some homogeneous catalysts for the decomposition of formic acid are summarized in Table 4.

Fukuzumi *et al.* reported that HCOOH selectively decomposed to afford H_2 and CO_2 in aqueous solution at room temperature in the presence of a catalytic amount of a water-soluble Rh catalyst, $[Rh^{III}(Cp^*)(bpy)(H_2O)](SO_4)$ (Cp^* = pentamethylcyclopentadienyl, bpy = 2,2′-bipyridine).[251] A similar non-phosphine catalyst $[Ir^{III}(Cp^*)(dhbpy)(H_2O)](SO_4)$ (Cp^* = pentamethylcyclopentadienyl, dhbpy = 4,4′-dihydroxy-2,2′-bipyridine) was reported by Himeda for generation of CO-free hydrogen from the decomposition of formic acid.[252] The highest catalytic activity (turnover frequency (TOF) of up to 14 000 h^{-1} at 90 °C) and an almost complete consumption of formic acid were obtained for the catalytic system. No deterioration of the catalyst was observed during the catalytic decomposition of HCOOH in the continuous runs of reaction. More recently, Fukuzumi *et al.* demonstrated that heteronuclear iridium–ruthenium complexes are highly active catalysts for hydrogen generation in an aqueous solution under ambient conditions giving a TOF of about 426 h^{-1}.[253]

In 2008, important investigations were made by two independent groups, Beller and Laurenczy *et al.*[30,242,254–258] Beller and coworkers investigated the decomposition of formic acid with different homogeneous catalysts at 40 °C, including $RhCl_3 \cdot xH_2O$, $RuBr_3 \cdot xH_2O$, $[\{RuCl_2(p\text{-cymene})\}_2]$, $[RuCl_2(PPh_3)_3]$, $[\{RuCl_2(benzene)_2\}_2]$, *etc.* in the presence of

Table 4 Performances of selected homogeneous catalysts for the decomposition of formic acid[a]

Catalyst (precursor) and ligands	TOF (h^{-1})	T (°C)	Ref.
$[Ru_2(m\text{-}CO)(CO)_4(m\text{-dppm})_2]$	500	RT	250
$RuBr_3 \cdot xH_2O$, 3 equiv. $(PPh)_3$	3630	40	242
$RuCl_2(PPh_3)_3$	2688	40	254
$[RuCl_2(benzene)]_2$, 6 equiv. dppe	900	40	257
$RuCl_3 \cdot xH_2O$, 2 equiv. TPPTS	460	120	30
$RuCl_3$, 2 equiv. *m*TPPDS	476	90	265
$[Rh^{III}(Cp^*)(H_2O)(bpy)]^{2+}$	28	RT	251
$[Ir^{III}(Cp^*)(H_2O)(bpm)Ru^{II}(bpy)_2]^{4+}$	426	RT	253
[Ir(Cp*)-4,4′-hydroxy-2,2′-bipyridine]	3100	60	252
	1.4×10^4	90	252
$[Ru_2(HCO_2)_2(CO)_4]$	1.8×10^4	120	266
$[Ru_4(CO)_{12}H_4]$	1470	107	267
$[\{RuCl_2(p\text{-cymene})\}_2]$	1540	80	268
$RuCl_3$	280	80	262
$[Fe(BF_4)_2] \cdot 6H_2O$, 2 equiv. PP_3	1942	40	264
	5390	80	264

[a] Abbreviations used: dppm = 1,1-bis(diphenylphosphino)methane, dppe = 1,2-bis(diphenylphosphino)ethane tppts = trisodium-3,3′,3″-phosphinidynetris(benzenesulfonate), tppds = ddiphenylphosphine disulfonate, bpy = 2,2′-bipyrdine, bpm = 2,2′-bipyrimidine, PP_3 = tris[(2-diphenylphosphino)ethyl] phosphine.

amine adducts.[242,254,255] They investigated the influence of different amines on catalytic activity by using 1000 ppm $[\{RuCl_2(p\text{-cymene})\}_2]$ as the standard catalyst precursor, and a formic acid to amine ratio of 5 : 2. Generally, for the reaction catalyzed by $[\{RuCl_2(p\text{-cymene})\}_2]$, various alkyl dimethylamines with longer alkyl chains showed a higher degree of reaction rate promotion. High decomposition rates (TOF = 21 h^{-1}) were also observed by using triethylamine.[242,255] Interestingly, using the ruthenium phosphine complex $[RuCl_2(PPh_3)_3]$ they observed much higher turnover frequencies: up to 417 and 302 h^{-1} after 2 and 3 hours, respectively, and a formic acid conversion of 90% after 3 hours.[254] A similar activity is obtained with an *in situ* catalyst prepared from ruthenium trichloride hydrate and triphenylphosphine in DMF. Among all examined catalysts under different reaction conditions, the decomposition of formic acid in a 5HCOOH–2NEt$_3$ mixture over the catalyst *in situ* prepared from $RuBr_3 \cdot xH_2O$ and three equivalents of PPh_3 after pretreatment in DMF at 80 °C for 2 h yielded an initial TOF of 3630 h^{-1} at 40 °C.[242] Recently, they developed a highly active and stable catalyst system (*in situ* generated (benzene)ruthenium dichloride dimer $[RuCl_2(benzene)]_2$/6 equiv. 1,2-bis(diphenylphosphino)ethane (dppe)) for both batch and continuous experiments. In the presence of this *in situ* generated catalyst and *N*,*N*-dimethyl-*n*-hexylamine a total TON of approximately 260 000, with an average TOF of more than 900 h^{-1}, at room temperature has been achieved. In the produced gas mixture only hydrogen and CO_2 are detected, which allows direct use in fuel cells after simple cleaning by a charcoal column.[257] In another report they demonstrated for the first time the light-accelerated hydrogen generation reaction from formic acid with a catalyst system based on a ruthenium precursor (*i.e.* $[RuCl_2(benzene)]_2$, $RuCl_3 \cdot xH_2O$, $[Ru(cod)(methylallyl)_2]$) and aryl phosphines (PPh_3, dppe *etc.*) (Fig. 10).[258] The best productivity is observed with a $[RuCl_2(benzene)]_2$/dppe catalyst, where gas evolution increased from 407 to 2804 turnovers, which is an almost 7-fold increase.

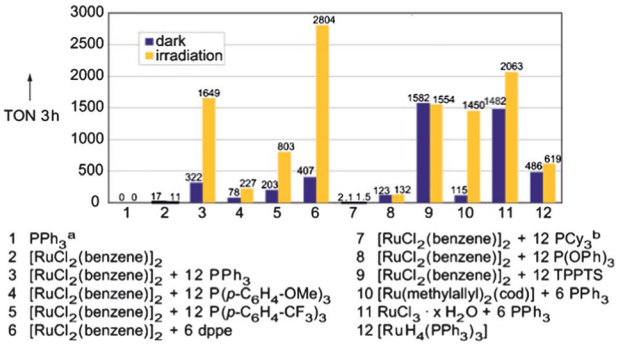

Fig. 10 The influence of light on the decomposition of 5 mL 5HCOOH–2NEt$_3$ with ruthenium catalyst systems (320 ppm Ru, 40 °C). (a) No hydrogen detected by GC; (b) no dark experiment, performed under lab conditions, environmental light. Reprinted with permission from ref. 258. Copyright 2009 Royal Society of Chemistry.

In 2008, Laurenczy and coworkers developed a homogenous catalytic system which can efficiently and selectively decompose formic acid into hydrogen and carbon dioxide.[30,256] $[Ru(H_2O)_6]^{2+}$, $[Ru(H_2O)_6]^{3+}$ and $RuCl_3 \cdot xH_2O$ were found to be excellent precatalysts in the presence of TPPTS (TPPTS = *meta*-trisulfonated triphenylphosphine) for the formic acid decomposition in the aqueous phase under mild conditions and over a large range of pressures. With increased temperatures, the reaction rate became much higher (TOF = 670 h^{-1} at 120 °C) and at all reaction temperatures, the conversion was higher than 90%. The performance of the catalytic system for continuous hydrogen generation is also investigated. A detailed mechanism study was also carried out by this group using multinuclear NMR spectroscopy.[256] They proposed a tentative reaction mechanism consisting of two competitive catalytic cycles involving a monohydride ruthenium complex $[RuH(tppts)_2(H_2O)_3]^+$ as a common intermediate. Furthermore, they developed heterogeneous catalysts based on ruthenium(II)–TPPTS catalyst using different immobilization/solidification methods, such as ion exchange, polymer immobilization and physical absorption.[259] Both ion exchange and coordination to the phosphine-containing polymers gave stable supported heterogeneous catalysts for selective decomposition of formic acid. The leaching of the metal was negligible and the catalysts could be easily separated from the reactant/solution, and could be reused directly.

The finding by Beller and co-workers showed that the high catalytic activity for formic acid decomposition was obtained with a high ratio of organic amine to formic acid. In the formic acid decomposition process developed by Laurenczy and co-workers, sodium formate (HCOONa) was used, which is non-volatile but only active at high temperature. Shi, Deng and co-workers realized that amine-functionalized ionic liquids (ILs), defined as organic salts with melting points below 100 °C, can be substituted for volatile organic amines.[260,261] They prepared and used a series of amine-functionalized ionic liquids for hydrogen generation by the selective catalytic decomposition of formic acid in the presence of $[\{RuCl_2(p\text{-cymene})\}_2]$ catalyst (Table 5).[261] Among the ILs investigated, the 1-(2-diisopropylaminoethyl)-3-methylimidazolium chloride–sodium formate (iPr$_2$NEMimCl–HCOONa) system exhibited high activity (TOF > 600 h^{-1}) at

Table 5 Decomposition of formic acid in the presence of different functionalized ionic liquids (ILs). Reaction conditions: 30.85 mmol formic acid (97%), 30.85 μmol $\{RuCl_2(p\text{-cymene})\}_2$, 60 °C, 2 h. V, gas volume of H_2 and CO_2. 1 h, 1 hour. 2 h, 2 hours

Catalysts	V_{1h}/V_{2h} (mL)[a]	TON_{1h}/TON_{2h}	Conv. (x%, 2 h)
H_2NEMImBr	9/17	3/6	1.1
Me_2NEMImCl	33/58	11/19	3.8
Me_2NPMImCl	28/51	9/17	1.4
Et_2NEMImCl	41/71	14/24	4.7
i-Pr_2NEMImCl	108/206	36/68	13.6
i-Pr_2NEMMImCl	156/311	52/103	20.6
i-Pr_2NEPyCl	113/210	37/70	13.9
i-Pr_2NEMImBF_4	52/87	17/29	5.8
i-Pr_2NEMImOTf	74/122	25/40	8.1
i-Pr_2NEMImNTf_2	35/55	12/18	3.6
i-Pr_2NEMImCl/HCOO[b]	207/445	69/147	29.5
Et_2NEMImCl–HCOONa[c]	172/331	57/110	21.9
i-Pr_2NEMImCl–HCOONa[d]	382/862	127/286	57.1
i-Pr_2NEPyCl–HCOONa[e]	252/455	84/151	30.1
i-Pr_2NEMImCl–HCOONa[f]	481/971	627/1267	64.3

[a] Measured by gas burette ($H_2 : CO_2 = 1 : 1$). [b] *i*-Pr_2NEMImCl : *i*-Pr_2NEMImHCOO = 88.2 : 11.8 (mol). [c] 5 mmol Et_2NEMImCl + 5 mmol HCOONa. [d] 5 mmol *i*-Pr_2NEMImCl + 5 mmol HCOONa. [e] 5 mmol *i*-Pr_2NEPyCl + 5 mmol HCOONa. [f] 10 mmol *i*-Pr_2NEMImCl + 5 mmol HCOONa, 7.84 μmol $[RuCl_2(p\text{-cymene})]_2$.[261,262]

60 °C. However, the authors stated that they were not able to recycle the catalyst solution. In a separate study Wasserscheid and coworkers investigated an outstanding simple, active and recyclable ionic liquid-based system for the catalytic decomposition of formic acid. The most efficient system, $RuCl_3$ dissolved in [EMMIM][OAc], was shown to produce hydrogen and carbon dioxide as the only products and was recyclable for at least nine cycles.[262] During these cycles no deactivation or change in selectivity was observed. It is worth noting that this simple catalytic system exhibits turnover frequencies of 150 h^{-1} at 80 °C and 850 h^{-1} at 120 °C.

Recently, Beller, Ludwig and coworkers reported the first non-noble metal-based homogeneous catalyst system for hydrogen generation from formic acid. By application of a catalyst formed *in situ* from inexpensive $Fe_3(CO)_{12}$, 2,2′ : 6′2″-terpyridine or 1,10-phenanthroline, and triphenylphosphine, hydrogen generation is possible under visible light irradiation and ambient temperature.[263] The best catalyst system identified was triirondodecacarbonyl ($Fe_3(CO)_{12}$) in the presence of triphenylphosphine (PPh_3), 2,2′ : 6′2″-terpyridine (tpy), and dimethylformamide (DMF). This system was capable of generating hydrogen from formic acid–amine adducts at temperatures above 100 °C, whereas in the presence of *in situ* generated catalyst system under visible light irradiation, hydrogen generation even occurred at room temperature. Depending on the kind of *N*-ligands significant catalyst turnover numbers (>100) and turnover frequencies (up to 200 h^{-1}) were observed, which are the highest known to date for non-precious metal catalyzed hydrogen generation from formic acid. NMR, IR and DFT studies of the iron complexes formed under reaction conditions confirm that PPh_3 plays an active role in the catalytic cycle and that *N*-ligands enhance the stability of the system. It was shown that the reaction mechanism includes iron hydride species which are generated exclusively under irradiation with visible light.

In another report in 2011, Beller, Ludwig, Laurenczy and coworkers demonstrated a highly active catalyst system based on iron complexes for the selective decomposition of formic acid (Table 6).[264] This catalyst consists of an iron cation that is permanently coordinated by four phosphorus centers of a tetradentate phosphine ligand, namely tris[(2-diphenylphosphino) ethyl] phosphine (PP_3). The remaining two coordination sites of the Fe^{II} center are occupied by the HCOOH substrate and/or product-derived species during the catalytic cycle. The catalyst can be formed *in situ* from $[Fe(BF_4)_2]$ and the PP_3 ligand under the reaction conditions or can be added to the reaction mixture in a presynthesized form as $[FeH(PP_3)]^+$. This catalyst functions in a common organic solvent (propylene carbonate) without any further additives or light. It achieves a high TON of up to 100 000 and a high TOF of nearly 10 000 h^{-1}. The catalyst shows high selectivity for H_2 formation, whereas the rate of the competing HCOOH decomposition pathway to CO and H_2O is negligible. Spectroscopic studies and density functional theory calculations suggest two viable pathways (I and II, Fig. 11) for H_2 release from HCOOH, both of which go through a common Fe-hydride species, $[FeH(PP_3)]^+$(**1**). In the first candidate of

Table 6 Hydrogen generation from 5 mL propylene carbonate solution of formic acid (containing 2 mL formic acid) in the presence of different Fe-complex/PP_3 catalysts (5.3 mmol [Fe] and 2 equiv. PP_3) at 40 °C. V, gas volume of H_2 and CO_2; 2 h, 2 hours; 3 h, 3 hours[264]

Catalysts	V_{2h} (mL)	V_{3h} (mL)	TON_{2h}	TON_{3h}
$[Fe(BF_4)_2]\cdot 6H_2O/PP_3$	146	215	562	825
$[Fe(BF_4)_2]\cdot 6H_2O/2PP_3$	333	505	71 279	1942
$[FeH(PP_3)]BF_4$	194	295	745	1135
$[FeH(PP_3)]BF_4/PP_3$	319	500	1227	1923
$[FeH(H_2)(PP_3)]BF_4$	189	294	727	1129
$[FeH(H_2)(PP_3)]BPh_4$	174	264	670	1015
$[FeCl(PP_3)]BF_4$	0.4	0.4	—	—

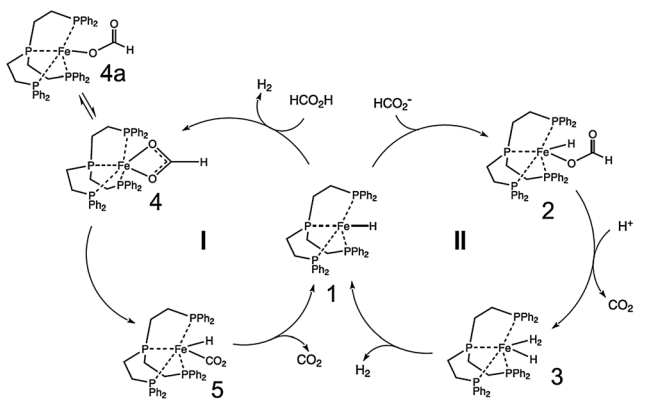

Fig. 11 Proposed mechanisms for the selective iron-catalyzed hydrogen generation from formic acid. Reprinted with permission from ref. 264. Copyright 2011 The American Association for the Advancement of Science.

catalytic cycle, the Fe-hydride combines with a proton from HCOOH, and H_2 is formed and released. The HCO_2^- counter anion remains coordinated to the Fe center and undergoes β-hydride elimination (transferring the hydride from HCO_2^- to Fe) in the rate-determining step; subsequent CO_2 release reforms $[FeH(PP_3)]^+$. In the second candidate of catalytic cycle, formate coordinates to $[FeH(PP_3)]^+$ to form a neutral $[FeH(HCO_2)(PP_3)]$ (**2**) species. β-Hydride elimination and protonation releases CO_2 and closes the catalytic cycle after H_2 release. The Fe center remains exclusively in the formal +2 oxidation state during both catalytic cycles.

6.1.2 Heterogeneous catalytic decomposition of formic acid. The decomposition of formic acid using heterogeneous catalysts has remained relatively underdeveloped despite several notable examples in the literature. Most of the studies have been performed in the gas phase[269–288] over catalysts of metals,[270–273] metal oxides,[274–279] and metal supported on oxides or carbon.[280–290] A gas phase reaction will require heating above 100 °C, the normal boiling point of formic acid, or introducing an inert carrier gas to dilute formic acid below its saturated vapor pressure. These constraints would add complexity to a hydrogen generation device. Therefore, it is highly desirable to develop heterogeneous catalysts for liquid-phase formic decomposition. In this direction, Williams *et al.* used Pd/C (1 wt% Pd) to obtain hydrogen from aqueous formic acid at room temperature.[279] In the approach of Sasson, Blum and coworkers in the mid-1980s, hydrogen was evolved from an aqueous sodium formate solution at 70 °C in the presence of a Pd/C catalyst (10 wt% Pd).[292] Table 7 summarizes selected heterogeneous catalysts for decomposition of aqueous formic acid.

Recently, Xing and coworkers developed carbon supported Pd–Cu, Pd–Ag and Pd–Au alloy catalysts and overcame the poisoning by CO byproduct from the decomposition of formic acid at low temperatures.[240] The best decomposition of formic acid/sodium formate was demonstrated by Pd–Au/C. They also found that the activities of Pd–Au/C and Pd–Ag/C can be markedly enhanced by co-deposition with CeO_2. The TOFs of Pd–Au/C–CeO_2 and Pd–Ag/C–CeO_2 are 227 and 76 h^{-1}, respectively, at 92 °C. Inspired by the promotion effect of Ce on Pd–Au/C and Pd–Ag/C catalysts, they extended their investigations to other rare earth elements (REs) (Dy, Eu, and Ho) and obtained TOFs 269 ± 202, 387 ± 292, 224 ± 73, and 45 ± 11 h^{-1} for Pd–Au–Dy/C, Pd–Au–Eu/C, Pd–Au–Ho/C and Pd–Au/C catalysts, respectively, at 92 °C.[293] In addition, these catalysts were even active at room temperature temporarily, and above 52 °C steadily. All the REs-promoted Pd–Au/C catalysts showed lower activation energies for decomposition of formic acid than Pd–Au/C and Pd–Au–Eu/C had the lowest value of 84.2 ± 7.4 kJ mol^{-1}. These authors have also developed a PdAu bimetallic catalyst with a PdAu@Au core–shell nanostructure supported on carbon, which shows higher activity than the monometallic counterparts.[294] In a report by Chan and coworkers, the metal–metal oxide catalyst composed of platinum ruthenium and bismuth, denoted as $PtRuBiO_x$, was found to catalyze selective dehydrogenation of formic acid in water at nearly ambient temperature.[295] The observed activation energy was 37.3 kJ mol^{-1} and the turnover frequency was estimated to be 312 h^{-1} in the first hour of the decomposition.

In an effort, Tsang and coworkers prepared various core–shell nanoparticles having an inner core of a metal element and an external shell of palladium (Table 8).[296,297] Among all metals tested, the highest activity toward formic acid decomposition at room temperature was found for Ag@Pd NPs (diameter 8 nm) with the thinnest continuous Pd shell (1–2 atomic layers) and corresponding Ag/Pd alloy and pure Pd catalysts show very low activity (Fig. 12).[296,297] Turnover frequencies per surface Pd site were comparable to homogeneous catalysts: 125 h^{-1} at 20 °C and

Table 7 Selected heterogeneous catalysts for the decomposition of aqueous formic acid

Catalyst	TOF (h^{-1})	T (°C)	Ref.
20 wt% PdAu/C	27	92	232
20 wt% PdAu/C–CeO_2	227	92	232
20 wt% Pd–Au–Dy/C	269	92	281
20 wt% Pd–Au–Eu/C	387	92	281
20 wt% Pd–Au–Ho/C	224	92	281
30 wt% $PtRuBiO_x$	312	80	283
20.4 wt% PdAu/MIL-101	—	90	286
Pd–S–SiO_2	803	85	300
Au@Pd/C(core–shell)	125	20	284
	626	90	284
2 wt% Au@SiO_2	—	90	287
0.8 wt% Au/ZrO_2	1590	50	301

Table 8 Results on the initial catalytic decomposition of formic acid in water. Reaction conditions: 1 M formic acid in 10 mL total volume; with temperature as specified; reaction time, 2 h (ref. 296)

Catalysts	Temp (°C)	H_2/CO_2	CO (ppm)	TOF (h^{-1})
Ag@Pd (1 : 1)	20	0.96	—	125
Ag@Pd (1 : 1)	35	0.98	—	156
Ag@Pd (1 : 1)	50	1.02	—	252
Ag@Pd (1 : 1)	70	1.03	74	500
Ag@Pd (1 : 1)	90	1.02	84	626
Ag/Pd alloy (1 : 1)	20	1.03	—	144
Pd (2.3 nm)	20	0.98	—	24
Pd (3.2 nm)	20	1.01	—	25
Ag@Pd/C (1 : 1)	20	1.09	—	192

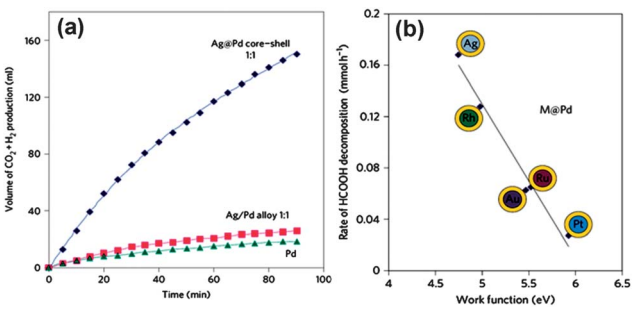

Fig. 12 (a) Time course plots of hydrogen generation from aqueous formic acid (10 mL of 1 M) in the presence of Ag@Pd, Ag–Pd alloy and pure Pd catalysts (2.0×10^{-4} mol, 0.021 g). (b) Correlation with the work function of the M core, where M = fcc (111) Ag, Rh, Au, Ru and Pt or hexagonal close-packed (hcp) (0001) Ru. Ag, with the largest difference in work function in relation to Pd, gives the strongest electron promotion to the Pd shell. Reprinted with permission from ref. 296. Copyright 2011 Nature Publishing Group.

252 h^{-1} at 50 °C. At 20 °C, an equimolar mixture of hydrogen and CO_2 was continuously produced without any trace of CO; on the other hand, CO was detected at temperatures higher than 50 °C. In contrast to previous reports on Pd catalysts, no deactivation was observed during the experiments, and the rate closely followed the first order kinetics of formic acid decomposition by reaction (29). Furthermore, theoretical calculations showing a strong correlation between the catalytic activity and the work function of the metal core: the largest net difference with the work function of the Pd shell will lead to the highest adsorption energy by charge transfer from the core to the shell, hence to the best possible activity of the resulting bimetallic structure for formic acid decomposition (Fig. 12b). The very short range of this so-called "ligand" electronic effect between the two metals explains why the highest performance is achieved for the thinnest Pd layer. Nanomaterials interface definitely plays a key role in catalysis.

Recently, we reported bimetallic Au–Pd NPs immobilized in mesoporous MOFs as efficient catalysts for decomposition of formic acid.[298] MIL-101 was chosen as a support because of its large pore sizes (2.9–3.4 nm) and window sizes (1.2–1.4 nm) and its hybrid pore surface, which facilitates the encapsulation of metal NPs and the adsorption of the catalytic substrate formic acid inside the pores. In order to improve the interactions between the metal precursors and the MIL-101 support, we grafted the electron-rich functional group ethylenediamine (ED) into MIL-101, which contains coordinatively unsaturated Cr^{3+} centers, to form ED–MIL-101, which exhibited improved immobilization of small metal NPs. The resulting bimetallic Au–Pd NPs immobilized in the MOF, MIL-101, and ethylenediamine (ED)–grafted MIL-101 (ED–MIL-101), Au–Pd/MIL-101 and Au–Pd/ED–MIL-101, represent the first highly active MOF-immobilized metal catalysts for the complete conversion of formic acid to hydrogen at a convenient temperature.

Very recently, we have developed a high-performance nanoreactor composed of silica nanospheres encapsulating amine-functionalized gold nanoparticles.[299] A microemulsion-templating approach was employed to fabricate gold nanoparticles encapsulated inside the hollow silica nanospheres using the procedure shown in Fig. 13. The gold@silica nanospheres synthesized under different conditions show distinct catalytic activities in the decomposition of formic acid in aqueous media. Similar to the monometallic gold nanoparticles supported on MOF or carbon, the gold nanoparticles encapsulated in SiO_2 nanospheres without amine functionalization ($Au@SiO_2$, prepared using TEOS and $HAuCl_4$; Fig. 13a) are inactive for the decomposition of aqueous formic acid. However, the gold nanoparticles encapsulated in amine-functionalized silica nanospheres, surprisingly, exhibit remarkable catalytic activities and 100% H_2 selectivity. At 90 °C, 139 mg of formic acid (3.0 mmol) can be completely converted to hydrogen (H_2) and carbon dioxide (CO_2), which were identified by mass spectrometry and gas chromatography, in 360 and 240 min in the presence of 60 mg of $Au@SiO_2$_EN (2 wt% Au; prepared using TEOS and $Au(en)_2Cl_3$; Fig. 13b) and $Au@SiO_2$_AP (2 wt% Au; prepared using TEOS/APTS and $HAuCl_4$; Fig. 13c), respectively (Fig. 14).

Remarkably, it is found that all the Au NPs supported on the outer surface of SiO_2 are inactive no matter whether the outer surface is functionalized with amine, indicating that the encapsulation of Au NPs in the amine-functionalized silica nanosphere is important for obtaining a suitable environment around the Au NPs for effective catalysis of formic acid decomposition. It should be noted that the amine-functionalized $Au@SiO_2$ nanosphere catalyst ($Au@SiO_2$_AP) keeps its catalytic activity for the four runs, showing a high stability/durability that is important for practical application of catalysts.

Very recently, Cao and coworkers demonstrated the selective dehydrogenation of FA–amine mixtures using ultradispersed subnanometric (~1.8 nm) gold as catalysts. The reaction catalyzed by Au subnanoclusters dispersed on acid-tolerant ZrO_2, proceeds efficiently and selectively under ambient conditions, without the generation of any unwanted byproduct, such as CO, They achieved a TOF of 1590 h^{-1} and TON of more than 118 400 at 50 °C.[301]

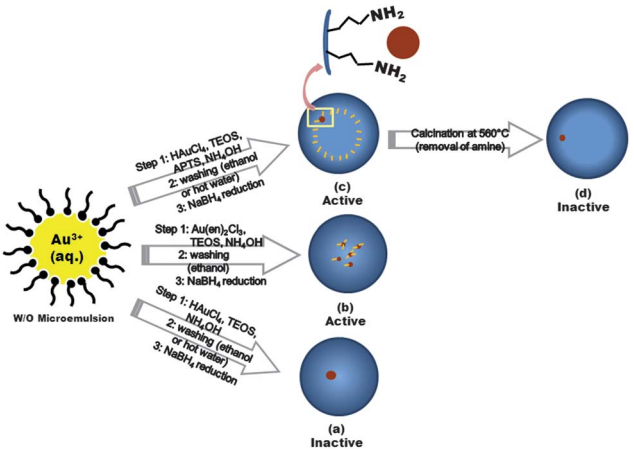

Fig. 13 Microemulsion-based syntheses of gold nanocatalysts encapsulated within hollow silica nanospheres of (a) $Au@SiO_2$, (b) $Au@SiO_2$_EN, (c) $Au@SiO_2$_AP, and (d) $Au@SiO_2$_AP_C. Reprinted with permission from ref. 299. Copyright 2012 Royal Society of Chemistry.

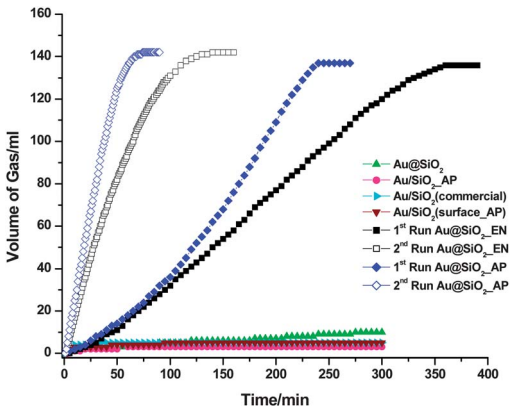

Fig. 14 Time-course plots for hydrogen generation from the aqueous solution (1.0 mL) of formic acid (3.0 M) and sodium formate (1.0 M) in the presence of different Au NP catalysts (60 mg, 2 wt% Au) at 90 °C. Reprinted with permission from ref. 299. Copyright 2012 Royal Society of Chemistry.

6.2. Synthesis of formic acid

Formic acid decomposition generates a major byproduct, carbon dioxide, that is a major green-house gas. For better hydrogen storage systems, efficient recycling of the byproduct has to be achieved. It has been proposed that the carbon dioxide can be reduced by molecular hydrogen to formic acid or methanol. Even if methanol has a higher storage capacity of two hydrogen molecules compared to one in formic acid, the use of carbon dioxide to synthesize formic acid should be preferred.[302] The need for three equivalents of hydrogen to produce one equivalent of methanol results in a loss of one equivalent of hydrogen, since water is formed. In contrast, a transfer rate of 100% for formic acid formation is found. Therefore, the reversible storage of hydrogen in formic acid by reduction of carbon dioxide is an efficient process.[291]

6.2.1 Reduction of CO_2 to formic acid by H_2. The synthesis of formic acid from reaction of CO_2 and H_2 is, however, thermodynamically unfavorable, since the reaction of CO_2 and H_2 to HCOOH is endergonic ($\Delta G^{\circ}_{298} = +33$ kJ mol^{-1}) [eqn (31)]. As observed for the selective decomposition of formic acid to carbon dioxide and hydrogen, this pathway also needs a suitable catalyst.[301] In general, the high temperature reaction of carbon dioxide and hydrogen results in the formation of carbon monoxide and water (the water gas shift reaction). For the formation of formic acid, the presence of a catalyst is needed in addition to certain conditions such as a base (inorganic or organic) to shift the reaction equilibria to the right side. Hydrogenation of CO_2 has been widely investigated by using both homogeneous and heterogeneous catalysts.

$$H_2 + CO_2 \rightarrow HCOOH\ \Delta G = +33\ \text{kJ mol}^{-1} \qquad (31)$$

The development of this reaction and the state-of-the art catalyst systems are well described in the literature.[303–305] Therefore, we will discuss some selective catalysts.

6.2.1.1 Homogeneous catalytic formation of formic acid. Extensive studies have been undertaken to develop the homogenous catalysis of hydrogenation of carbon dioxide to yield formic acid. Numerous transition metal complexes based on *e.g.* Ru, Rh, Ir, Pd, Ni, Fe, Ti, and Mo have demonstrated excellent activities.[303–312] Table 9 summarizes some of the most active homogenous catalytic systems for hydrogenation of carbon dioxide. The activity of catalysts significantly depends on the pH of the reaction solution.[311–315] An excellent activity is feasible in the presence of a base, because the abstraction of protons forces the reaction, which is in contrast to the thermodynamically unfavorable "base-free" reduction. In organic media, amines are preferred, whereas in water, NaOH or carbonates are used.

Interestingly, the removal of the base is not essential, since the adduct of formic acid and base allows the straightforward decomposition to hydrogen. Besides this, the reaction outcome can be improved by applying supercritical conditions, due to the high availability of carbon dioxide, while in the solution approach the solubility of carbon dioxide is the limiting factor. One of the most active systems has been invented by Jessop and co-workers.[306] A turnover frequency (TOF) of 95 000 h^{-1} was achieved by [RuCl(OAc)(PMe$_3$)$_4$] under supercritical conditions

Table 9 Formation of formic acid by reduction of CO_2 in the presence of some homogeneous catalysts[a]

Catalysts	TOF (h^{-1})	T (°C)	Ref.
[RuCl(OAc)(PMe$_3$)$_4$]	95 000	50	306
[RuCl$_2$(tppms)$_2$]$_2$	9600	80	307
[RhCl(tppts)$_3$]	7260	81	305
[RuH$_2$(PMe$_3$)$_4$]	1400	50	308
[Rh(hfacac)(dcpb)]	1335	25	309
[(PNP)IrH$_3$]	73 000	120	310
[Cp*Ir(dhbipy)Cl]	42 000	120	311
[Cp*Ir(dhpt)Cl]	33 000	120	311
[{Cp*Ir(Cl)}$_2$(thbpym)]	53 800	80	312

[a] Abbreviation used: tppms = 3-sulfonatophenyldiphenylphosphine, tppts = trisodium-3,3′,3″-phosphinidynetris(benzenesulfonate), hfacac = hexafluoroacetylacetonate, dcpb = 1,4-di(dicyclohexylphosphino) butane, PNP = PNP-type pincer ligand, dhbipy = 4,4′-dihydroxy-2,2′-bipyrdine, dhpt = 4,7-dihydroxy-1,10-phenantroline, thbpym = 4,4′,6,6′-tetrahydroxy-2,2′-bipyrimidine.

(CO_2-pressure: 190 bar, temperature: 50 °C). The group of Joó reported a [RuCl$_2$(tppms)$_2$]$_2$ (tppms = *meta*-monosulfonated triphenylphosphine) catalyst with a TOF value of 9600 h^{-1},[307] with which the reaction was carried out under non-supercritical conditions (CO_2-pressure: 95 bar, temperature: 80 °C) in water. Leitner and co-workers reported that the complex Rh(hfacac)(dcpb) (hfacac = hexafluoroacetylacetonate; dcpb = 1,4-di(dicyclohexylphosphino)butane) demonstrated an outstanding activity of 1335 h^{-1} (TOF) at room temperature and a low CO_2–H_2 pressure (40 atm).[309]

An approach for reversible hydrogen storage using CO_2 and H_2 has been demonstrated by Hull, Himeda, Fujita and coworkers (Fig. 15).[312] Herein, a water-soluble, pH-modulated catalyst drives the hydrogenation of CO_2 to formate under basic conditions, and hydrogen release is easily triggered by acidifying the solution to protonate the catalyst. Progress has been reported in this regard by Himeda and coworker using [Cp*IrCl] complexes with 4,4′-dihydroxy-2,2′-bipyrdine (dhbipy) and 4,7-dihydroxy-1,10-phenanthroline (dhpt) ligands.[311] They observed significantly higher activities of these complexes with TOFs of 42 000, and 33 000 h^{-1}. It has been demonstrated that the hydroxy groups on the aromatic bipyridine and phenanthroline ligands have an enormous effect on the Lewis basicity of the ligand and, hence, on the metal center and its catalytic activity – when the ligand is protonated, the catalyst is inactive. The

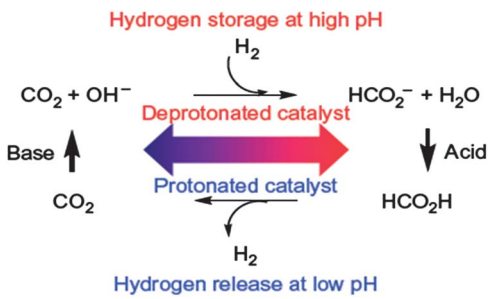

Fig. 15 Reversible H_2 storage is achieved by switching the pH to protonate or deprotonate the catalyst. Reprinted with permission from ref. 312. Copyright 2012 Nature Publishing Group.

deprotonated hydroxypyridine ligand, for example, forms a pyridinolate, which is a much stronger σ-donor than the protonated pyridinol, which can be tuned by changing the pH value of the reaction solution.[313] The pH-dependent activation and deactivation of the catalyst also has an effect on the reusability of the catalyst: in acidic media, the catalyst precipitates and can thus be separated from the reaction mixture. Very recently, Hull, Himeda, Fujita and coworkers developed a binuclear iridium catalyst containing [Cp*IrCl] and 4,4′,6,6′-tetrahydroxy-2,2′-bipyrimidine (thbpym) ligand, the first catalyst capable of reversible H_2 storage using CO_2 in aqueous media under mild temperatures and pressures.[312] A recyclable pressurization sequence demonstrates that low-pressure (atmospheric) H_2 gas can be stored as liquid formate, and then used to generate high-pressure H_2 and CO_2 for possible fuel applications. The –OH moieties on the thbpym ligand are pH-responsive, and H_2 storage can be turned on or off by adjusting the pH of the solution. The rate of CO_2 hydrogenation was as high as 70 h^{-1} (25 °C and 0.1 MPa) and 53 800 h^{-1} (80 °C and 5 MPa). This catalyst was also very active for the decomposition of formic acid or formate to give CO-free H_2 and CO_2 at low pH with a TOF of 158 000 at 80 °C and 228 000 h^{-1} at 90 °C.

Very recently, Fukuzumi and cowrkers reported a organo-iridium complex, $[Ir^{III}(Cp^*)(4\text{-}(1H\text{-pyrazol-1-yl-}\kappa N^2)\text{benzoic acid-}\kappa C^3)(H_2O)]_2SO_4$, as an efficient catalyst for interconversion between H_2 and HCOOH depending on pH. Hydrogenation of carbon dioxide by hydrogen occurs in the presence of a catalyst in weakly basic water (pH 7.5) under an atmospheric pressure of H_2 and CO_2 at room temperature, whereas formic acid efficiently decomposes to afford H_2 and CO_2 in the presence of the same catalyst in acidic water (pH 2.8).[316]

6.2.1.2 Heterogeneous catalytic formation of formic acid. There are only a few reports on the direct conversion of carbon dioxide to form formic acid with heterogeneous catalysts. Possible reasons are the unfavorable reaction conditions (high temperature, high pressure) compared to homogeneous catalysts and low chemoselectivity of heterogeneous processes, as formic acid can act as an intermediate to form methanol or methane.[317–321] The first attempt for synthesis of formic acid over heterogeneous catalyst was reported as early as 1935.[322] The reactions were carried out with RANEY® nickel as catalyst under 200–400 bar hydrogen pressure and 80–150 °C. However, one equivalent of amine had to be added in order to shift the thermodynamic equilibrium towards the formation of the product formic acid.

Recently, Fachinetti and coworkers developed a heterogeneous gold catalyst for synthesis of formic acid by hydrogenation of carbon dioxide.[323] They found gold black catalyst promotes the CO_2 hydrogenation in the presence of neat NEt_3 to form $HCOOH/NEt_3$ adducts. A continuous production process for catalyst- and solvent-free adducts has been demonstrated using a robust Au/TiO_2 (AUROlite) catalyst and production of 1.326 kg (7.365 mol) $HCOOH–NEt_3$ adduct with an acid/amine ratio of 1.7 has been achieved from CO_2–H_2 (1 : 1) and NEt_3 in the presence of 13 g AUROlite (Au = 0.7 mmol) catalyst in a steel net cage in 37 days. The adducts have been split into pure HCOOH (anhydrous) and neat NEt_3 with the help of high-boiling tri-*n*-hexylamine $(n\text{-}C_6H_{13})_3N$.

The reduction of carbonates to formic acid under mild reaction conditions was demonstrated by Wiener *et al.* applying Pd/C as catalyst.[324] However, due to the chemical equilibrium between carbonate and formate the reaction could not be run to completeness. Further problems are the decrease of the solubility of carbonate with increasing formate concentration and the separation of the product from the reaction mixture.

Inspired by high activity of homogeneous catalysts, some immobilized catalysts have also been investigated. Ruthenium complexes immobilized over amine-functionalized silica have been developed with an *in situ* synthetic approach for CO_2 hydrogenation to formic acid.[325] The catalyst not only exhibits high activity (TOF = 1384 h^{-1}) and 100% selectivity, but also offers practical advantages such as easy separation and recycling.

Ionic liquids have some unique properties, such as excellent thermal stability, wide liquid regions, and favorable solvation properties for various substances. Han and coworkers reported that the combination of a basic ionic liquid [mammim][OTf] (1-(*N*,*N*-dimethylaminoethyl)-2,3-dimethylimidazolium trifluoromethane-sulfonate) and a silica-supported ruthenium complex ("Si"–$(CH_2)_3$–$NH(CSCH_3)$–$RuCl_3$–PPh_3) promoted CO_2 hydrogenation to formic acid with satisfactory activity and selectivity.[326] At a total pressure of 18 bar ($H_2 : CO_2 = 1 : 1$) a maximum TOF of 103 h^{-1} was achieved. The activity has been proven to be constant over 5 cycles.

In addition to thermal catalytic reactions, electrochemical reduction of carbon dioxide on an amalgamated nickel cathode has been performed for production of formic acid by Williams and co-workers. While the maximal energetic efficiency is 60% and the concentration of formic acid is limited to 4 mol L^{-1}, further improvement is expected.[291]

6.2.2 Photochemical and enzymatic reductions of CO_2 to formic acid. The photochemical and enzymatic reductions of CO_2 are potential green technologies for the synthesis of organic compounds from CO_2 as the starting material. Many studies on CO_2 fixation or utilization have been performed in detail. However, the quantum yields and selectivity of products based on the reduction of CO_2 are still low.[327–331] Formic acid is the simplest carboxylic acid and is produced by the two-electron reduction of CO_2. In artificial photocatalytic CO_2 reduction, CO_2 can be only reduced to CO under an existing methodology. On the other hand, it has been known that formate dehydrogenase (FDH) enzymes can catalyze the reversible conversion of formic acid to CO_2. Thus, in principle, the synthesis of formic acid from CO_2 by using visible light and FDH has been developed. NADH- (nicotinamide adenine dinucleotide) dependent enzymes can be used to reduce the formed *N*,*N*′-alkyl-4,4′- or -2,2′-bipyridinium salt molecules as an artificial substrate instead of NADH or NAD^+. For example, FDH from *Saccharomyces cerevisiae* is a NADH-dependent enzyme and uses the various reduced forms of the bipyridinium salt molecules as a substrate for the conversion of CO_2 to formic acid.

Willner and coworkers reported the enzymatic formic acid synthesis from HCO_3^- with FDH and photoreduction of various 4,4′- or 2,2′-bipyridinium salts by a system containing $[Ru(bpy)_3]^{2+}$ (bpy = 2,2′-bipyridine) as a photosensitizer and mercaptoethanol (RSH) as an electron donor (Fig. 16a).[332–335] The efficiency of formic acid synthesis depends on the nature of

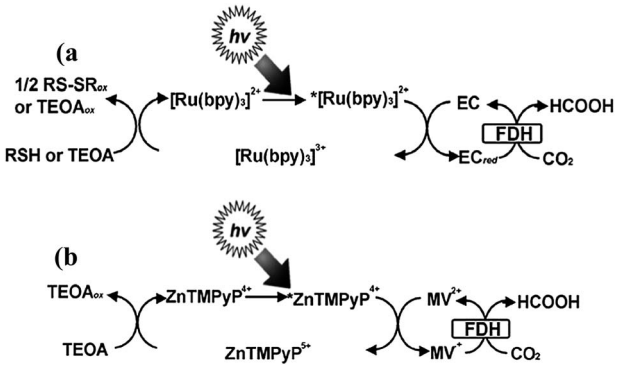

Fig. 16 Photochemical and enzymatic CO_2 conversion to formic acid (a) with a system consisting of an electron donor (RSH or TEOA), $[Ru(bpy)_3]^{2+}$, bipyridinium salt (EC) and FDH, and (b) with a system consisting of TEOA, $ZnTMPyP^{4+}$, bipyridinium salt (MV^{2+}), and FDH. Reprinted with permission from ref. 331. Copyright 2011 Wiley-VCH.

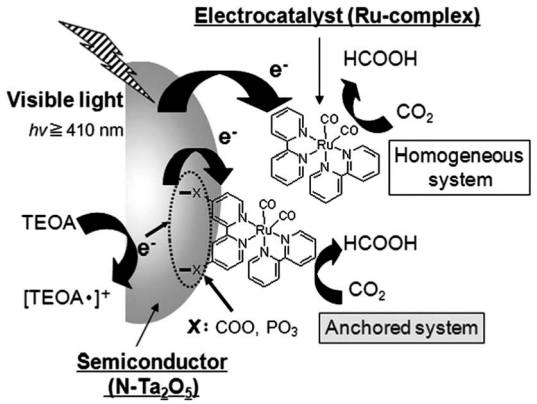

Fig. 17 Mechanism for the reduction of CO_2 by photocatalysis under visible-light with an Ru-complex and an N–Ta_2O_5 hybrid catalyst. Reprinted with permission from ref. 345. Copyright 2011 Royal Society of Chemistry.

the bipyridinium salts, and the quantum yield for formic acid from HCO_3^- is in the range of 0.5–1.6%.

In a report from Kodaka *et al.*, direct formic acid synthesis from CO_2 gas with the system consisting of triethanolamine (TEOA), $[Ru(bpy)_3]^{2+}$, various bipyridinium salts (1,1′-dialkyl-4,4′-bipyridinium salts or 1,1′-dialkyl-2,2′-bipyridinium salts), and FDH has also been described (Fig. 16a).[336] They investigated the effects of the structure and redox potentials of various bipyridinium salts on the synthesis of formic acid from CO_2. After 7 h irradiation, the formation of formic acid in the concentration range of 0.2–0.95 mM was achieved from a sample solution containing 0.5 M TEOA, 0.5 mM $[Ru(bpy)_3]^{2+}$, 3.0 mM bipyridinium salt, and 8 mg FDH. The most effective formic acid synthesis from CO_2 was observed by using *N*,*N*′-trimethylene-2,2′-bipyridinium salt and the yield depends on the relative magnitude of the redox potentials of the bipyridinium salts.

To develop a methodology for the conversion of CO_2 to formic acid with FDH by visible light sensitization, the dye molecule should possess a high sensitization activity. In this regard, the synthesis of formic acid from HCO_3^- with FDH and the photoreduction of *N*,*N*′-dimethyl-4,4′-bipyridinium (MV^{2+}) with systems using water soluble zinc porphyrins (zinc tetrakis-(4-methylpyridyl)porphyrin, ZnTMPyP) have been introduced by Amao and Miyatani.[337–339] $ZnTMPyP^{4+}$ has been used as a photosensitizer, as shown in Fig. 16b. After 3 h irradiation, the formation of 60 μM of formic acid was achieved from the sample solution containing 0.3 M TEOA, 9.0 μM $ZnTMPyP^{4+}$, 15 mM MV^{2+}, 20 units FDH and 1.0 mM $NaHCO_3$. The conversion yield of HCO_3^- to formic acid was estimated to be 6%. Later, they used Mg chlorophyll-a (MgChl-a) as visible light photosensitizer.[340] The sample solution in this case consisted of NADPH, MgChl-a, MV^{2+}, FDH, and CO_2 gas. When the sample solution containing NADPH (3.0 mM), MgChl-a (9.0 μM), MV^{2+} (0.1 mM), FDH (5 units), and CO_2 gas (saturated) was irradiated at 30 °C, 56 μm of formic acid was produced after 4 h of irradiation. Further, it has been observed that formic acid was not produced in the absence of any one of the components.

Sato and coworkers reported immobilization of a molecular CO_2 reduction catalyst onto a semiconductor surface for engineering hybrid photocatalytic materials.[341–345] The ruthenium catalysts were grafted onto different *p*-type semiconductors such as N-doped Ta_2O_5, Z-doped InP, *etc.* *via* covalent linkages or *via* a polymerization process. It was reported that the robustness of a hybrid system depends strongly on the choice of grafting linkages. The $[Ru(dpbpy)(bpy)(CO)_2]$/N–Ta_2O_5 (dpbpy = 4,4′-diphosphonate-2,2′-bipyridine, bpy = 2,2′-bipyridine) system with phosphate linker displayed a 5 times higher rate of CO_2 reduction to HCOOH (in acetonitrile solution using visible light) compared with the $[Ru(dcbpy)(bpy)(CO)_2]$/N–Ta_2O_5 (dcbpy: 4,4′-dicarboxy-2,2′-bipyridine, bpy = 2,2′-bipyridine) system with carbonate linker (Fig. 17).[341,345] By using a Deronzier's-type ruthenium bipyridine-based polymeric film catalyst, a robust system adapted for working in aqueous solution was achieved.[344]

Recently Sato, Arai and coworkers reported that the photoelectrochemical reduction of CO_2 to $HCOO^-$ (formate) over a p-type InP/Ru complex polymer hybrid photocatalyst was highly enhanced by introducing an anchoring complex into the polymer (Fig. 18).[343] By functionally combining the hybrid photocatalyst with TiO_2 for water oxidation, selective photoreduction of CO_2 to $HCOO^-$ was achieved in aqueous media, in which H_2O was used as both an electron donor and a proton source. The

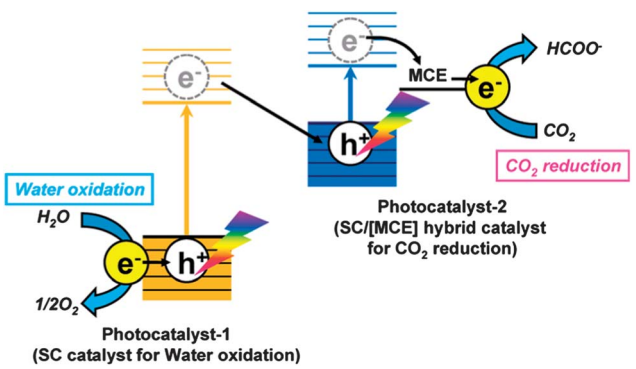

Fig. 18 Total reaction of the Z-scheme system for CO_2 reduction. Reprinted with permission from ref. 343. Copyright 2011 American Chemical Society.

so-called Z-scheme (or two-step photoexcitation) system operated with no external electrical bias. The selectivity for $HCOO^-$ production was >70%, and the conversion efficiency of solar energy to chemical energy was 0.03–0.04%.

6.3 Conclusions

Formic acid, having 4.4 wt% hydrogen content, represents a convenient hydrogen carrier in fuel cells designed for portable use. A power supply system could be feasibly based on the catalytic processes of formation and decomposition of formic acid. The present scenario of catalytic decomposition and formation of formic acid shows the presence of many effective homogeneous and heterogeneous catalysts. To meet practical applications, further work is needed for the development of low-cost, more efficient catalysts, especially heterogeneous catalysts. Moreover, development of photocatalytic systems for both the processes (fixation and the evolution of hydrogen to/from formic acid), which employs sustainable/renewable energy resources, is highly desirable.

7. Other liquid organic hydogen storage materials

Hydrogen storage in liquid organic hydrogen carriers (LOHCs) has attracted much attention in the past few decades because of its simple, safe, and feasible handling of hydrogen.[346–360] The concept of hydrogen storage in LOHCs is based on reversible catalytic hydrogenation–dehydrogenation reactions. First, the hydrogen is chemically stored in an organic carrier through a catalytic hydrogenation reaction. When the demand for energy exists, the hydrogen is extracted from the organic carrier by a catalytic dehydrogenation reaction and fed into fuel cells to generate electricity. The practical barrier for LOHCs is appreciably lower than for other storage media because they are chemically similar to the current distribution medium, gasoline. The tanks, piping and refinery systems used to make and deliver gasoline are appropriate for LOHCs. Therefore, a number of research efforts have been resulted in the development of various liquid organic carriers for hydrogen storage.[346–360] Initial efforts to develop liquid organic hydrogen carriers were primarily focused on cycloalkanes.[346–351] The dehydrogenation of these cheap, abundant materials to the corresponding aromatic compounds releases approximately 7 wt% hydrogen. However, the large enthalpy of dehydrogenation of cycloalkanes (~60 kJ mol^{-1} H_2) is a major drawback to their utilization in practical systems. Pez *et al.* calculated the enthalpy of formation of hydrogenation for a variety of aromatic heterocycles and their saturated analogs.[352,353] Their calculations show that the ΔH of dehydrogenation is significantly lowered upon introduction of a hetero-atom into the ring system as it significantly reduces the aromaticity of the dehydrogenated molecule. This led several groups to explore the reversible dehydrogenation of heterocyclic aromatic compounds as *N*-ethyl perhydrocarbazole to ethylcarbazole.[352–360] Although promising hydrogen cycling performances have been demonstrated, these investigators utilized very high loadings of heterogeneous, precious metal catalysts in order to achieve acceptable dehydrogenation kinetics at temperatures (≤150 °C) near the operating temperatures of PEM fuel cells. The high cost of the massive quantities of precious metals precludes the commercialization of these systems.

8. Conclusions and perspective

Safe, efficient storage and delivery of hydrogen is essential for the development of a hydrogen-based energy infrastructure. All the liquid-phase chemical hydrogen storage materials reviewed above have relatively high hydrogen content and have the potential to be used as hydrogen sources suitable for portable fuel cells. However, each of them has its own merits and drawbacks. The materials and systems presented herein can effectively work under mild conditions (even at room temperature) with suitable catalysts compared to the hydrogen generation from organic compounds (for example, various cyclohexane derivatives and alcohols as feedstock) and thermolysis systems of solid-state chemical hydrogen storage materials, which usually need high temperature reforming or decomposition processes. Easy recharging using liquid filling pumps and the availability of the current infrastructure of liquid fuels for recharging as well as the production of only nitrogen/carbon dioxide, which does not need on-board collection for recycling, besides hydrogen, of hydrous hydrazine and formic acid as hydrogen storage materials, are extraordinary advantages over solid-state hydrogen storage materials. Furthermore, the development of chemical hydrogen storage materials containing abundant elements (C, H and O for formic acid, and H and N for hydrazine) is encouraging in comparison to much less abundant boron-containing hydrogen storage materials. From these points of view, hydrous hydrazine and formic acid, which contain only abundant elements, do not need on-board collection of spent fuel for recycling, and can be easily recharged, are suitable for large-scale automotive application, while boron-containing materials, which contain less abundant elements and need for on-site collection of spent fuel for recycling, are suitable for small-scale, mobile single-use devices where reusability is not important. Recent research efforts have greatly improved the hydrogen generation temperature and the reaction kinetics in these systems and, especially, intensive efforts have been made to develop low-cost non-noble metal catalysts, which is important for implementation of hydrogen storage as a global energy solution. However, for practical applications in mobile electric devices, limitations are still pending, such as, cost, catalyst deactivation, regeneration of byproducts, and control of the reaction kinetics. Further developments of these systems will certainly contribute to the establishment of future sustainable energy infrastuctures.

We have tried to present an up-to-date overview in such a rapidly growing field, while the subject is very active and many papers are contributed each year (even during the writing of this article) from chemists, physical and materials scientists, *etc.* Therefore, it is hard to take into account all publications to this field in our limited number of pages. We apologize here if some significant contributions were left out.

Acknowledgements

The authors gratefully acknowledge the reviewers for valuable comments and constructive suggestions. The authors are pleased to acknowledge the fine work of the talented and dedicated

graduate students, postdoctoral fellows, and colleagues who have worked with us in this area and whose names can be found in the references. The authors would like to thank National Institute of Advanced Industrial Science and Technology (AIST) and Japan Society for the Promotion of Science (JSPS) for financial support. M. Y. thanks JSPS for postdoctoral fellowship.

References

1 A. W. C. van den Berg and C. O. Areán, *Chem. Commun.*, 2008, 668–681.
2 *Hydrogen as a Future Energy Carrier*, ed. A. Züttel, A. Borgschulte and L. Schlapbach, Wiley-VCH, Weinheim, 2008.
3 L. Schlapbach and A. Zuttel, *Nature*, 2001, **414**, 353–358.
4 Fuel Cell Technologies Program, http://www1.eere.energy.gov/hydrogenandfuelcells/mypp/.
5 G. Ferey, *Nature*, 2005, **436**, 187–188.
6 S. Orimo, Y. Nakamori, J. R. Eliseo, A. Züttel and C. M. Jensen, *Chem. Rev.*, 2007, **107**, 4111–4132.
7 N. L. Rosi, J. Eckert, M. Eddaoudi, D. T. Vodak, J. Kim, M. O'Keeffe and O. M. Yaghi, *Science*, 2003, **300**, 1127–1129.
8 A. M. Seayad and D. M. Antonelli, *Adv. Mater.*, 2004, **16**, 765–777.
9 G. A. Deluga, J. R. Salge, L. D. Schmidt and X. E. Verykios, *Science*, 2004, **303**, 993–997.
10 P. Makowski, A. Thomas, P. Kuhn and F. Goettmann, *Energy Environ. Sci.*, 2009, **2**, 480–490.
11 Y. G. Wang, N. Shah and G. P. Huffman, *Catal. Today*, 2005, **99**, 359–364.
12 U. Eberle, M. Felderhoff and F. Schüth, *Angew. Chem., Int. Ed.*, 2009, **48**, 6608–6630.
13 P. Chen, Z. T. Xiong, J. Z. Luo, J. Y. Lin and K. L. Tan, *Nature*, 2002, **420**, 302–304.
14 B. Bogdanovic and M. Schwickardi, *J. Alloys Compd.*, 1997, **253–254**, 1–9.
15 W. Grochala and P. P. Edwards, *Chem. Rev.*, 2004, **104**, 1283–1316.
16 M. Chandra and Q. Xu, *J. Power Sources*, 2006, **156**, 190–194.
17 Q. Xu and M. Chandra, *J. Power Sources*, 2006, **163**, 364–370.
18 H. L. Jiang, S. K. Singh, J. M. Yan, X. B. Zhang and Q. Xu, *ChemSusChem*, 2010, **3**, 541–549.
19 P. Wang and X. D. Kang, *Dalton Trans.*, 2008, 5400–5413.
20 T. Umegaki, J. M. Yan, X. B. Zhang, H. Shioyama, N. Kuriyama and Q. Xu, *Int. J. Hydrogen Energy*, 2009, **34**, 2303–2311.
21 F. H. Stephens, V. Pons and R. T. Baker, *Dalton Trans.*, 2007, 2613–2626.
22 C. W. Hamilton, R. T. Baker, A. Staubitz and I. Manners, *Chem. Soc. Rev.*, 2009, **38**, 279–293.
23 H. W. Langmi and G. S. McGrady, *Coord. Chem. Rev.*, 2007, **251**, 925–935.
24 J. Hannauer, O. Akdim, U. B. Demirci, C. Geantet, J. M. Herrmann, P. Miele and Q. Xu, *Energy Environ. Sci.*, 2011, **4**, 3355–3358.
25 U. B. Demirci and P. Miele, *Energy Environ. Sci.*, 2011, **4**, 3334–3341.
26 S. K. Singh, X. B. Zhang and Q. Xu, *J. Am. Chem. Soc.*, 2009, **131**, 9894–9895.
27 S. K. Singh and Q. Xu, *J. Am. Chem. Soc.*, 2009, **131**, 18032–18033.
28 F. Joó, *ChemSusChem*, 2008, **1**, 805–808.
29 (*a*) B. Loges, A. Boddien, F. Gartner, H. Junge and M. Beller, *Top. Catal.*, 2010, **53**, 902–914; (*b*) M. Grasemann and G. Laurenczy, *Energy Environ. Sci.*, 2012, **5**, 8171–8181; (*c*) A. Boddien, C. Federsel, P. Sponholz, D. Mellmann, R. Jackstell, H. Junge, G. Laurenczy and M. Beller, *Energy Environ. Sci.*, 2012, **5**, 8907–8911.
30 C. Fellay, P. J. Dyson and G. Laurenczy, *Angew. Chem., Int. Ed.*, 2008, **47**, 3966–3968.
31 E. Y. Marrero-Alfonso, A. M. Beaird, T. A. Davis and M. A. Matthews, *Ind. Eng. Chem. Res.*, 2009, **48**, 3703–3712.
32 B. H. Liu and Z. P. Li, *J. Power Sources*, 2009, **187**, 527–534.
33 H. I. Schlesinger, H. C. Brown, A. B. Finholt, J. R. Gilbreath, H. R. Hockstra and E. K. Hydo, *J. Am. Chem. Soc.*, 1953, **75**, 215–219.
34 U. B. Demirci and P. Miele, *C. R. Chim.*, 2009, **12**, 943–950.
35 Y. Nakamori, H. W. Li, M. Matsuo, K. Miwa, S. Towata and S. Orimo, *J. Phys. Chem. Solids*, 2008, **69**, 2292–2296.
36 S. C. Amendola, S. L. Sharp-Goldman, M. S. Janjua, N. C. Spencer, M. T. Kelly, P. J. Petillo and M. Binder, *Int. J. Hydrogen Energy*, 2000, **25**, 969–975.
37 S. C. Amendola, S. L. Sharp-Goldman, M. S. Janjua, M. T. Kelly, P. J. Petillo and M. Binder, *J. Power Sources*, 2000, **85**, 186–189.
38 Y. Shang and R. Chen, *Energy Fuels*, 2006, **20**, 2142–2148.
39 J. H. Wee, K. Y. Lee and S. H. Kim, *Fuel Process. Technol.*, 2006, **87**, 811–819.
40 E. Fakioglu, Y. Yurum and N. T. Veziroglu, *Int. J. Hydrogen Energy*, 2004, **29**, 1371–1376.
41 H. C. Brown and C. A. Brown, *J. Am. Chem. Soc.*, 1962, **84**, 1493–1494.
42 S. Suda, Y. M. Sun, B. H. Liu, Y. Zhou, S. Morimitsu, K. Arai, N. Tsukamoto, M. Uchida, Y. Candra and Z. P. Li, *Appl. Phys. A: Mater. Sci. Process.*, 2001, **72**, 209–212.
43 Y. Kojima, K. Suzuki, K. Fukumoto, M. Sasaki, T. Yamamoto and Y. Kawai, *Int. J. Hydrogen Energy*, 2002, **27**, 1029–1034.
44 P. P. Prosini and P. Gislon, *J. Power Sources*, 2006, **161**, 290–293.
45 S. Murugesan and V. R. Subramanian, *J. Power Sources*, 2009, **187**, 216–223.
46 E. Keçeli and S. Özkar, *J. Mol. Catal. A: Chem.*, 2008, **286**, 87–91.
47 C. M. Kaufman and B. Sen, *J. Chem. Soc., Dalton Trans.*, 1985, 307–313.
48 A. Levy, J. B. Brown and C. J. Lyons, *Ind. Eng. Chem.*, 1960, **52**, 211–214.
49 K. A. Holbrook and P. J. Twist, *J. Chem. Soc. A*, 1971, 890–894.
50 R. Paul, P. Buisson and N. Joseph, *Ind. Eng. Chem.*, 1952, **44**, 1006–1010.
51 G. Guella, B. Patton and A. Miotello, *J. Phys. Chem. C*, 2007, **111**, 18744–18750.
52 U. B. Demirci and F. Garin, *J. Alloys Compd.*, 2008, **463**, 107–111.
53 T. F. Hung, H. C. Kuo, C. W. Tsai, H. M. Chen, R. S. Liu, B. J. Weng and J. F. Lee, *J. Mater. Chem.*, 2011, **21**, 11754–11759.
54 U. B. Demirci, O. Akdim, J. Andrieux, J. Hannauer, R. Chamoun and P. Miele, *Fuel Cells*, 2010, **10**, 335–350.
55 C. W. Tsai, H. M. Chen, R. S. Liu, J. F. Lee, S. M. Chang and B. J. Weng, *Int. J. Hydrogen Energy*, 2012, **37**, 3338–3343.
56 M. Zahmakiran and S. Özkar, *J. Mol. Catal. A: Chem.*, 2006, **258**, 95–103.
57 V. I. Simagina, P. A. Storozhenko, O. V. Netskina, O. V. Komova, G. V. Odegova, T. Yu. Samoilenko and A. G. Gentsler, *Kinet. Catal.*, 2007, **48**, 168–175.
58 U. B. Demirci and F. Garin, *Catal. Commun.*, 2008, **9**, 1167–1172.
59 B. H. Liu, Z. P. Li and S. Suda, *J. Alloys Compd.*, 2006, **415**, 288–293.
60 S. U. Jeong, R. K. Kim, E. A. Cho, H. J. Kim, S. W. Nam, I. H. Oh, S. A. Hong and S. H. Kim, *J. Power Sources*, 2005, **144**, 129–134.
61 Ö. Metin and S. Özkar, *Int. J. Hydrogen Energy*, 2007, **32**, 1707–1715.
62 J. H. Park, P. Shakkthivel, H. J. Kim, M. K. Han, J. H. Jang, Y. R. Kim, H. S. Kim and Y. G. Shu, *Int. J. Hydrogen Energy*, 2008, **33**, 1845–1852.
63 P. Krishnan, T. H. Yang, W. Y. Lee and C. S. Kim, *J. Power Sources*, 2005, **143**, 17–23.
64 P. Krishnan, K. L. Hsueh and S. D. Yim, *Appl. Catal., B*, 2007, **77**, 206–214.
65 M. Zahmakiran and S. Özkar, *Langmuir*, 2009, **25**, 2667–2678.
66 C. Wu, F. Wu, Y. Bai, B. Yi and H. Zhang, *Mater. Lett.*, 2005, **59**, 1748–1751.
67 J. C. Walter, A. Zurawski, D. Montgomery, M. Thornburg and S. Revankar, *J. Power Sources*, 2008, **179**, 335–339.
68 N. Patel, G. Guella, A. Kale, A. Miotello, B. Patton, C. Zanchetta, L. Mirenghi and P. Rotolo, *Appl. Catal., A*, 2007, **323**, 18–24.
69 N. Patel, R. Fernandes, G. Guella, A. Kale, A. Miotello, B. Patton and C. Zanchetta, *J. Phys. Chem. C*, 2008, **112**, 6968–6976.
70 D. Hua, Y. Hanxi, A. Xinping and C. Chuansin, *Int. J. Hydrogen Energy*, 2003, **28**, 1095–1100.
71 O. Akdim, U. B. Demirci, D. Muller and P. Miele, *Int. J. Hydrogen Energy*, 2009, **34**, 2631–2637.
72 S. U. Jeong, E. A. Cho, S. W. Nam, I. H. Oh, U. H. Jung and S. H. Kim, *Int. J. Hydrogen Energy*, 2007, **32**, 1749–1754.
73 X. Yuan, C. Jia, X. L. Ding and Z. F. Ma, *Int. J. Hydrogen Energy*, 2012, **37**, 995–1001.

74 D. Xu, P. Dai, X. Liu, C. Cao and Q. Guo, *J. Power Sources*, 2008, **182**, 616–620.
75 H. B. Dai, Y. Liang, P. Wang and H. M. Cheng, *J. Power Sources*, 2008, **177**, 17–23.
76 H. B. Dai, Y. Liang, P. Wang, X. D. Yao, T. Rufford, M. Lu and H. M. Cheng, *Int. J. Hydrogen Energy*, 2008, **33**, 4405–4412.
77 K. W. Cho and H. S. Kwon, *Catal. Today*, 2007, **120**, 298–304.
78 J. H. Park, P. Shakkthivel, H. J. Kim, M. K. Han, J. H. Jang, Y. R. Kim, H. S. Kim and Y. G. Shu, *Int. J. Hydrogen Energy*, 2008, **33**, 1845–1852.
79 C. Wu, H. Zhang and B. Yi, *Catal. Today*, 2004, **93–95**, 477–483.
80 W. Ye, H. Zhang, D. Xu, L. Ma and B. Yi, *J. Power Sources*, 2007, **164**, 544–548.
81 A. J. Hung, S. F. Tsai, Y. Y. Hsu, J. R. Ku, Y. H. Chen and C. C. Yu, *Int. J. Hydrogen Energy*, 2008, **33**, 6205–6215.
82 C. T. F. Lo, K. Karan and B. R. Davis, *Ind. Eng. Chem. Res.*, 2007, **46**, 5478–5484.
83 H. C. Brown, E. J. Mead and B. C. S. Rao, *J. Am. Chem. Soc.*, 1955, **77**, 6209–6213.
84 R. E. Davis and J. A. Gottbrath, *J. Am. Chem. Soc.*, 1962, **84**, 895–898.
85 J. Hannauer, U. B. Demirci, G. Pastor, C. Geantet, J. M. Herrmann and P. Miele, *Energy Environ. Sci.*, 2010, **3**, 1796–1803.
86 J. Andrieux, U. B. Demirci, J. Hannauer, C. Gervais, C. Goutaudier and P. Miele, *Int. J. Hydrogen Energy*, 2011, **36**, 224–233.
87 J. Hannauer, U. B. Demirci, C. Geantet, J. M. Herrmann and P. Miele, *Phys. Chem. Chem. Phys.*, 2011, **13**, 3809–3818.
88 E. Y. Marrero-Alfonso, J. R. Gray, T. A. Davis and M. A. Matthews, *Int. J. Hydrogen Energy*, 2007, **32**, 4723–4730.
89 B. H. Liu, Z. P. Li and S. Suda, *J. Alloys Compd.*, 2009, **468**, 493–498.
90 US Department of Energy, *Office of Energy Efficiency and Renewable Energy and the Freedom CAR and Fuel Partnership, "Targets for Onboard Hydrogen Storage Systems for Light-Duty Vehicles"*, September 2009, http://www1.eere.energy.gov.
91 J. Yang, A. Sudik, C. Wolverton and D. J. Siegel, *Chem. Soc. Rev.*, 2010, **39**, 656–675.
92 H. K. Atiyeh and B. R. Davis, *Int. J. Hydrogen Energy*, 2007, **32**, 229–236.
93 Ç. Çakanyildirim and M. Gürü, *Int. J. Hydrogen Energy*, 2008, **33**, 4634–4639.
94 Y. Wu, M. T. Kelly and J. V. Ortega, *Review of Chemical Processes for the Synthesis of Sodium Borohydride*, 2007, http://205.254.148.40/hydrogenandfuelcells/pdfs/review_chemical_processes.pdf.
95 C. H. Liu, B. H. Chen, D. J. Lee, J. R. Ku and F. Tsau, *Ind. Eng. Chem. Res.*, 2010, **49**, 9864–9869.
96 G. Broja and W. Schlabacher, *DE Pat.*, 1108670, 1959.
97 T. Haga and Y. Kojima, *JP Pat.*, 2002–241109, 2002.
98 Y. Kojima and T. Haga, *Int. J. Hydrogen Energy*, 2003, **28**, 989–993.
99 Z. P. Li, B. H. Liu, N. Morigasaki and S. Suda, *J. Alloys Compd.*, 2003, **354**, 243–247.
100 Z. P. Li, N. Morigazaki, B. H. Liu and S. Suda, *J. Alloys Compd.*, 2003, **349**, 232–236.
101 A. Roine, *HSC Chemistry: V5.0*, Outokompu Research Oy, *Pori*, 2004.
102 S. C. Amendola and M. T. Kelly, *US Pat.*, 6433129, 2002.
103 S. C. Amendola, M. T. Kelly, J. V. Ortega and Y. Wu, *US Pat.*, 6670444, 2003.
104 S. C. Amendola, M. T. Kelly and Y. Wu, *US Pat.*, 6524542, 2003.
105 J. V. Ortega, Y. Wu, S. C. Amendola and M. T. Kelly, *US Pat.*, 6586563, 2003.
106 *Production of the Boranes and Related Research*, ed. R. T. Holzmann, Academic Press, New York, 1967.
107 O. Glemser, *DE Pat.*, 949943, 1956.
108 H. B. H. Cooper, *US Pat.*, 3734842, 1973.
109 D. M. F. Santos and C. A. C. Sequeira, *Int. J. Hydrogen Energy*, 2010, **35**, 9851–9861.
110 D. L. Calabretta and B. R. Davis, *J. Power Sources*, 2007, **164**, 782–791.
111 Q. Xu and M. Chandra, *J. Alloys Compd.*, 2007, **446–447**, 729–732.
112 A. Gutowska, L. Li, Y. Shin, C. M. Wang, X. S. Li, J. C. Linehan, R. S. Smith, B. D. Kay, B. Schmid, W. Shaw, M. Gutowski and T. Autrey, *Angew. Chem., Int. Ed.*, 2005, **44**, 3578–3582.
113 Z. Li, G. Zhu, G. Lu, S. Qiu and X. Yao, *J. Am. Chem. Soc.*, 2010, **132**, 1490–1491.
114 F. H. Stephens, R. T. Baker, M. H. Matus, D. J. Grant and D. A. Dixon, *Angew. Chem., Int. Ed.*, 2007, **46**, 746–749.
115 T. B. Marder, *Angew. Chem., Int. Ed.*, 2007, **46**, 8116–8118.
116 U. B. Demirci and P. Miele, *Energy Environ. Sci.*, 2009, **2**, 627–637.
117 http://www.eere.energy.gov/hydrogenandfuelcells/pdfs/freedomcar_targets_explanations.pdf.
118 R. Custelcean and Z. A. Dreger, *J. Phys. Chem. B*, 2003, **107**, 9231–9235.
119 S. G. Shore and R. W. Parry, *J. Am. Chem. Soc.*, 1958, **80**, 8–12.
120 A. T. Raissi, *Hydrogen From Ammonia and Ammonia–Borane Complex for Fuel Cell Applications*, Proceedings of the 2002 US DOE Hydrogen Program Review, 2002, http://www1.eere.energy.gov/hydrogenandfuelcells/pdfs/32405b15.pdf.
121 S. G. Shore and R. W. Parry, *J. Am. Chem. Soc.*, 1955, **77**, 6084–6085.
122 M. G. Hu, J. M. Van Paasschen and R. A. Geanangel, *J. Inorg. Nucl. Chem.*, 1977, **39**, 2147–2150.
123 P. V. Ramachandran and P. D. Gagare, *Inorg. Chem.*, 2007, **46**, 7810–7817.
124 E. Mayer, *Inorg. Chem.*, 1972, **11**, 866–869.
125 S. G. Shore and K. W. Boeddeker, *Inorg. Chem.*, 1964, **3**, 914–915.
126 R. A. Adams, J. Beres, A. Dodds and A. J. Morabito, *Inorg. Chem.*, 1971, **10**, 2072–2074.
127 M. E. Bluhm, M. G. Bradley, R. Butterick III, U. Kusari and L. G. Sneddon, *J. Am. Chem. Soc.*, 2006, **128**, 7748–7749.
128 L. Li, X. Yao, C. H. Sun, A. J. Du, L. N. Cheng, Z. H. Zhu, C. Z. Yu, J. Zou, S. C. Smith, P. Wang, H. M. Cheng, R. L. Frost and G. Q. M. Lu, *Adv. Funct. Mater.*, 2009, **19**, 265–271.
129 Z. T. Xiong, C. K. Yong, G. T. Wu, P. Chen, W. Shaw, A. Karkamkar, T. Autrey, M. O. Jones, S. R. Johnson, P. P. Edwards and W. I. F. David, *Nat. Mater.*, 2007, **7**, 138–141.
130 H. V. K. Diyabalanage, R. P. Shrestha, T. A. Semelsberger, B. L. Scott, M. E. Bowden, B. L. Davis and A. K. Burrell, *Angew. Chem., Int. Ed.*, 2007, **46**, 8995–8997.
131 V. Sit, R. A. Geanangel and W. W. Wendlandt, *Thermochim. Acta*, 1987, **113**, 379–382.
132 P. E. de Jongh and P. Adelhelm, *ChemSusChem*, 2010, **3**, 1332–1348.
133 C. A. Jaska, K. Temple, A. J. Lough and I. Manners, *J. Am. Chem. Soc.*, 2003, **125**, 9424–9434.
134 S. K. Kim, W. S. Han, T. J. Kim, T. Y. Kim, S. W. Nam, M. Mitoraj, L. Piekoś, A. Michalak, S. J. Hwang and S. O. Kang, *J. Am. Chem. Soc.*, 2010, **132**, 9954–9955.
135 M. Chandra and Q. Xu, *J. Power Sources*, 2006, **159**, 855–860.
136 T. J. Clark, G. R. Whittell and I. Manners, *Inorg. Chem.*, 2007, **46**, 7522–7527.
137 S. B. Kalidindi, M. Indirani and B. R. Jagirdar, *Inorg. Chem.*, 2008, **47**, 7424–7429.
138 F. Durap, M. Zahmakıran and S. Özkar, *Appl. Catal., A*, 2009, **369**, 53–59.
139 S. B. Kalidindi, A. A. Vernekar and B. R. Jagirdar, *Phys. Chem. Chem. Phys.*, 2009, **11**, 770–775.
140 M. Couturier, J. L. Tucker, B. M. Andresen, P. Dubé and J. T. Negri, *Org. Lett.*, 2001, **3**, 465–467.
141 P. A. Storozhenko, R. A. Svitsyn, V. A. Ketsko, A. K. Buryak and A. V. Ul'yanov, *Russ. J. Inorg. Chem.*, 2005, **50**, 980–985.
142 J. S. Wang and R. A. Geanangel, *Inorg. Chim. Acta*, 1988, **148**, 185–190.
143 M. Chandra and Q. Xu, *J. Power Sources*, 2007, **168**, 135–142.
144 F. Durap, M. Zahmakıran and S. Özkar, *Int. J. Hydrogen Energy*, 2009, **34**, 7223–7230.
145 O. Metin, S. Sxahin and S. Özkar, *Int. J. Hydrogen Energy*, 2009, **34**, 6304–6313.
146 M. Zahmakıran and S. Özkar, *Appl. Catal., B*, 2009, **89**, 104–110.
147 M. Rakap and S. Özkar, *Int. J. Hydrogen Energy*, 2010, **35**, 1305–1312.
148 J. M. Yan, X. B. Zhang, S. Han, H. Shioyama and Q. Xu, *Angew. Chem., Int. Ed.*, 2008, **47**, 2287–2289.
149 J. M. Yan, X. B. Zhang, S. Han, H. Shioyama and Q. Xu, *Inorg. Chem.*, 2009, **48**, 7389–7393.
150 T. Umegaki, J. M. Yan, X. B. Zhang, H. Shioyama, N. Kuriyama and Q. Xu, *Int. J. Hydrogen Energy*, 2009, **34**, 3816–3822.
151 J. M. Yan, X. B. Zhang, S. Han, H. Shioyama and Q. Xu, *J. Power Sources*, 2009, **194**, 478–481.
152 T. Umegaki, J. M. Yan, X. B. Zhang, H. Shioyama, N. Kuriyama and Q. Xu, *J. Power Sources*, 2009, **191**, 209–216.

153 Y. Li, L. Xie, Y. Li, J. Zheng and X. Li, *Chem.–Eur. J.*, 2009, **15**, 8951–8954.
154 J. M. Yan, X. B. Zhang, H. Shioyama and Q. Xu, *J. Power Sources*, 2010, **195**, 1091–1094.
155 T. Umegaki, J. M. Yan, X. B. Zhang, H. Shioyama, N. Kuriyama and Q. Xu, *J. Power Sources*, 2010, **195**, 8209–8214.
156 Ö. Metin, V. Mazumder, S. Özkar and S. Sun, *J. Am. Chem. Soc.*, 2010, **132**, 1468–1469.
157 C. Y. Cao, C. Q. Chen, W. Li, W. G. Song and W. Cai, *ChemSusChem*, 2010, **3**, 1241–1244.
158 P. Song, Y. Li, W. Li, B. He, J. Yang and X. Li, *Int. J. Hydrogen Energy*, 2011, **36**, 10468–10473.
159 P. Z. Li, K. Aranishi and Q. Xu, *Chem. Commun.*, 2012, **48**, 3173–3175.
160 M. Zahmakıran, F. Durap and S. Özkar, *Int. J. Hydrogen Energy*, 2010, **35**, 187–197.
161 R. Yi, R. Shi, G. Gao, N. Zhang, X. Cui, Y. He and X. Liu, *J. Phys. Chem. C*, 2009, **113**, 1222–1226.
162 H. L. Jiang, T. Umegaki, T. Akita, X. B. Zhang, M. Haruta and Q. Xu, *Chem.–Eur. J.*, 2010, **16**, 3132–3137.
163 Z. H. Lu, H. L. Jiang, M. Yadav, K. Aranishia and Q. Xu, *J. Mater. Chem.*, 2012, **22**, 5065–5071.
164 J. M. Yan, X. B. Zhang, T. Akita, M. Haruta and Q. Xu, *J. Am. Chem. Soc.*, 2010, **132**, 5326–5327.
165 K. Aranishi, H. L. Jiang, T. Akita, M. Haruta and Q. Xu, *Nano Res.*, 2011, **4**, 1233–1241.
166 H. L. Jiang, T. Akita and Q. Xu, *Chem. Commun.*, 2011, **47**, 10999–11001.
167 Y. Yamada, K. Yano, Q. Xu and S. Fukuzumi, *J. Phys. Chem. C*, 2010, **114**, 16456–16462.
168 Y. Yamada, K. Yano and S. Fukuzumi, *Energy Environ. Sci.*, 2012, **5**, 5356–5363.
169 H. Erdoğan, Ö. Metin and S. Özkar, *Phys. Chem. Chem. Phys.*, 2009, **11**, 10519–10525.
170 S. Çalışkan, M. Zahmakıran and S. Özkar, *Appl. Catal., B*, 2010, **93**, 387–394.
171 M. C. Denney, V. Pons, T. J. Hebden, D. M. Heinekey and K. I. Goldberg, *J. Am. Chem. Soc.*, 2006, **128**, 12048–12049.
172 R. J. Keaton, J. M. Blacquiere and R. T. Baker, *J. Am. Chem. Soc.*, 2007, **129**, 1844–1845.
173 R. P. Shrestha, H. V. K. Diyabalanage, T. A. Semelsberger, K. C. Ott and A. K. Burrell, *Int. J. Hydrogen Energy*, 2009, **34**, 2616–2621.
174 S. Kim, T. Kim, T. Kim, G. Lee, J. T. Park, S. W. Nam and S. O. Kang, *Chem. Commun.*, 2012, **48**, 2021–2023.
175 W. R. H. Wright, E. R. Berkeley, L. R. Alden, R. T. Baker and L. G. Sneddon, *Chem. Commun.*, 2011, **47**, 3177–3179.
176 M. Diwan, V. Diakov, E. Shafirovich and A. Varma, *Int. J. Hydrogen Energy*, 2008, **33**, 1135–1141.
177 M. Diwan, D. Hanna and A. Varma, *Int. J. Hydrogen Energy*, 2010, **35**, 577–584.
178 S. Basu, M. Diwan, M. G. Abiad, Y. Zheng, O. H. Campanella and A. Varma, *Int. J. Hydrogen Energy*, 2010, **35**, 2063–2072.
179 W. Luo, P. G. Campbell, L. N. Zakharov and S. Y. Liu, *J. Am. Chem. Soc.*, 2011, **133**, 19326–19329.
180 S. G. Shore and R. W. Parry, *J. Am. Chem. Soc.*, 1958, **80**, 8–12.
181 S. Hausdorf, F. Baitalow, G. Wolf and F. O. R. L. Mertens, *Int. J. Hydrogen Energy*, 2008, **33**, 608–614.
182 B. L. Davis, D. A. Dixon, E. B. Garner, J. C. Gordon, M. H. Matus, B. Scott and F. H. Stephens, *Angew. Chem., Int. Ed.*, 2009, **48**, 6812–6816.
183 A. D. Sutton, B. L. Davis, K. X. Bhattacharyya, B. D. Ellis, J. C. Gordon and P. P. Power, *Chem. Commun.*, 2010, **46**, 148–149.
184 A. D. Sutton, A. K. Burrell, D. A. Dixon, E. B. Garner III, J. C. Gordon, T. Nakagawa, K. C. Ott, J. P. Robinson and M. Vasiliu, *Science*, 2011, **331**, 1426–1429.
185 N. Mohajeri, A. T. Raissi and O. Adebiyi, *J. Power Sources*, 2007, **167**, 482–485.
186 G. P. Rachiero, U. B. Demirci and P. Miele, *Catal. Today*, 2011, **170**, 85–92.
187 G. P. Rachiero, U. B. Demirci and P. Miele, *Int. J. Hydrogen Energy*, 2011, **36**, 7051–7065.
188 C. G. Salentine, *Inorg. Chem.*, 1983, **22**, 3920–3924.
189 U. Sanyal, U. B. Demirci, B. R. Jagirdar and P. Miele, *ChemSusChem*, 2011, **4**, 1731–1739.
190 C. H. Liu, Y. C. Wu, C. C. Chou, B. H. Chen, C. L. Hsueh, J. R. Ku and F. Tsau, *Int. J. Hydrogen Energy*, 2009, **48**, 2950–2959.
191 H. I. Schlesinger, H. C. Brown, D. L. Mayfield and J. R. Gilbreath, *J. Am. Chem. Soc.*, 1953, **75**, 213–215.
192 H. I. Schlesinger, H. C. Brown and A. E. Finholt, *J. Am. Chem. Soc.*, 1953, **75**, 205–209.
193 L. G. Sneddon, *Amineborane Based Chemical Hydrogen Storage, DoE Hydrogen Annual Merit Review*, 2007, http://www.hydrogen.energy.gov/pdfs/review07/st_27_sneddon.pdf.
194 F. M. Taylor and J. Dewing, *US Pat.*, 3103417, 1963.
195 *Primer on Spontaneous Heating and Pyrophoricity, DOE Handbook*,1994, vol. 1081–1094, p. 16, http://www.hss.energy. gov/nuclearsafety/techstds/standard/hdbk1081/hdbk, 1081.pdf.
196 E. W. Schmidt, *Hydrazine and Its Derivatives: Preparation, Properties, Applications*, John Wiley & Sons, New York, 2nd edn, 1984.
197 M. Zheng, R. Cheng, X. Chen, N. Li, L. Li, X. Wang and T. Zhang, *Int. J. Hydrogen Energy*, 2005, **30**, 1081–1089.
198 X. Chen, T. Zhang, L. Xia, T. Li, M. Zheng, Z. Wu, X. Wang, Z. Wei, Q. Xin and C. Li, *Catal. Lett.*, 2002, **79**, 21–25.
199 M. Zheng, X. Chen, R. Cheng, N. Li, J. Sun, X. Wang and T. Zhang, *Catal. Commun.*, 2006, **7**, 187–191.
200 X. Chen, T. Zhang, P. Ying, M. Zheng, W. Wu, L. Xia, T. Li, X. Wang and C. Li, *Chem. Commun.*, 2002, 288–289.
201 J. B. O. Santos, G. P. Valença and J. A. J. Rodrigues, *J. Catal.*, 2002, **210**, 1–6.
202 W. E. Armstrong, L. B. Ryland and H. H. Voge, *US Pat.*, 4 124 538, 1978.
203 X. Chen, T. Zhang, M. Zheng, Z. Wu, W. Wu and C. Li, *J. Catal.*, 2004, **224**, 473–478.
204 Y. K. Al-Haydari, J. M. Saleh and M. H. Matloob, *J. Phys. Chem.*, 1985, **89**, 3286–3290.
205 D. J. Alberas, J. Kiss, Z. M. Liu and J. M. White, *Surf. Sci.*, 1992, **278**, 51–61.
206 J. Prasad and J. L. Gland, *Langmuir*, 1991, **7**, 722–726.
207 S. J. Cho, J. Lee, Y. S. Lee and D. P. Kim, *Catal. Lett.*, 2006, **109**, 181–187.
208 S. K. Singh and Q. Xu, *Inorg. Chem.*, 2010, **49**, 6148–6152.
209 S. K. Singh and Q. Xu, *Chem. Commun.*, 2010, **46**, 6545–6547.
210 S. K. Singh, Y. Iizuka and Q. Xu, *Int. J. HydrogenEnergy*, 2011, **36**, 11794–11801.
211 S. K. Singh, Z. H. Lu and Q. Xu, *Eur. J. Inorg. Chem.*, 2011, 2232–2237.
212 S. K. Singh, A. K. Singh, K. Aranishi and Q. Xu, *J. Am. Chem. Soc.*, 2011, **133**, 19638–19641.
213 J. Wang, X. B. Zhang, Z. L. Wang, L. M. Wang and Y. Zhang, *Energy Environ. Sci.*, 2012, **5**, 6885–6888.
214 L. He, Y. Huang, A. Wang, X. Wang, X. Chen, J. J. Delgado and T. Zhang, *Angew. Chem., Int. Ed.*, 2012, **48**, 4800–4803.
215 A. M. Cao and G. Veser, *Nat. Mater.*, 2009, **9**, 75–81.
216 R. Ferrando, J. Jellinek and R. L. Johnston, *Chem. Rev.*, 2008, **108**, 845–910.
217 H. Hayashi, *Res. Chem. Intermed.*, 1998, **24**, 183–196.
218 N. Hazari, *Chem. Soc. Rev.*, 2010, **39**, 4044–4056.
219 J. M. Chin, R. R. Schrock and P. Müller, *Inorg. Chem.*, 2010, **49**, 7904–7916.
220 V. Smil, in *Enriching the Earth: Fritz Haber, Carl Bosch and the Transformation of World Food Production*, MIT Press, Cambridge, MA, 2004.
221 T. Murakami, T. Nishikiori, T. Nohira and Y. Ito, *J. Am. Chem. Soc.*, 2003, **125**, 334–335.
222 S. Sridhar, T. Srinivasan, U. Virendra and A. A. Khan, *Chem. Eng. J.*, 2003, **94**, 51–56.
223 H. Hayashi, *Catal. Rev. Sci. Eng.*, 1990, **32**, 229–277.
224 S. Karahan, M. Zahmakiran and S. Özkar, *Int. J. Hydrogen Energy*, 2011, **36**, 4958–4966.
225 V. S. Nguyen, S. Swinnen, J. Leszczynski and M. T. Nguyen, *Phys. Chem. Chem. Phys.*, 2011, **13**, 6649–6656.
226 R. Moury, G. Moussa, U. B. Demirci, J. Hannauer, S. Bernard, E. Petit, A. Lee and P. Miele, *Phys. Chem. Chem. Phys.*, 2012, **14**, 1768–1777.
227 T. Hügle, M. F. Kühnel and D. Lentz, *J. Am. Chem. Soc.*, 2009, **131**, 7444–7446.
228 D. Çelik, S. Karahan, M. Zahmakıran and S. Özkar, *Int. J. Hydrogen Energy*, 2012, **37**, 5143–5151.

229 S. Karahan, M. Zahmakıran and S. Özkar, *Dalton Trans.*, 2012, **41**, 4912–4918.
230 J. H. Sinfelt, *Acc. Chem. Res.*, 1977, **10**, 15–20.
231 J. H. Sinfelt, *Acc. Chem. Res.*, 1987, **20**, 134–139.
232 Ç. Çakanyıldırım, U. B. Demirci, T. Şener, Q. Xu and P. Miele, *Int. J. Hydrogen Energy*, 2012, **37**, 9722–9729.
233 V. J. Goubeau and E. Ricker, *Z. Anorg. Allg. Chem.*, 1961, **310**, 123–142.
234 F. C. Gunderloy Jr, *Inorg. Chem.*, 1963, **2**, 221–222.
235 F. C. Gunderloy Jr, *Inorg. Synth.*, 1967, **9**, 13–16.
236 F. C. Gunderloy Jr and M. Park, *US Pat.*, 3375087, 1968.
237 A. Sutton, J. C. Gordon, K. C. Ott and A. K. Burrell, *US Pat.*, 2010/0272622, 2010.
238 J. R. Hyde and M. Poliakoff, *Chem. Commun.*, 2004, 1482–1483.
239 J. Zhang, P. G. Blazecka, M. M. Bruendl and Y. Huang, *J. Org. Chem.*, 2009, **74**, 1411–1414.
240 X. Zhou, Y. Huang, W. Xing, C. Liu, J. Liao and T. Lu, *Chem. Commun.*, 2008, 3540–3542.
241 T. C. Johnson, D. J. Morris and M. Wills, *Chem. Soc. Rev.*, 2010, **39**, 81–88.
242 A. Boddien, B. Loges, H. Junge and M. Beller, *ChemSusChem*, 2008, **1**, 751–758.
243 B. Loges, A. Boddien, F. Gartner, H. Junge and M. Beller, *Top. Catal.*, 2010, **53**, 902–914.
244 R. S. Coffey, *Chem. Commun.*, 1967, 923–924.
245 S. H. Strauss, K. H. Whitmire and D. F. Shriver, *J. Organomet. Chem.*, 1979, **174**, C59–C62.
246 R. S. Paonessa and W. C. Trogler, *J. Am. Chem. Soc.*, 1982, **104**, 3529–3530.
247 R. B. King and N. K. Battacharyya, *Inorg. Chim. Acta*, 1995, **237**, 65–69.
248 J. H. Shin, D. G. Churchill and G. Parkin, *J. Organomet. Chem.*, 2002, **642**, 9–15.
249 Y. Gao, J. Kuncheria, G. P. A. Yap and R. J. Puddephatt, *Chem. Commun.*, 1998, 2365–2366.
250 Y. Gao, J. K. Kuncheria, H. A. Jenkins, R. J. Puddephatt and G. P. A. Yap, *J. Chem. Soc., Dalton Trans.*, 2000, 3212–3217.
251 S. Fukuzumi, T. Kobayashi and T. Suenobu, *ChemSusChem*, 2008, **1**, 827–834.
252 Y. Himeda, *Green Chem.*, 2009, **11**, 2018–2022.
253 S. Fukuzumi, T. Kobayashi and T. Suenobu, *J. Am. Chem. Soc.*, 2010, **132**, 1496–1497.
254 B. Loges, A. Boddien, H. Junge and M. Beller, *Angew. Chem., Int. Ed.*, 2008, **47**, 3962–3965.
255 H. Junge, A. Boddien, F. Capitta, B. Loges, J. R. Noyes, S. Gladiali and M. Beller, *Tetrahedron Lett.*, 2009, **50**, 1603–1606.
256 C. Fellay, N. Yan, P. J. Dyson and G. Laurenczy, *Chem.–Eur. J.*, 2009, **15**, 3752–3760.
257 A. Boddien, B. Loges, H. Junge, F. Gartner, J. R. Noyes and M. Beller, *Adv. Synth. Catal.*, 2009, **351**, 2517–2520.
258 B. Loges, A. Boddien, H. Junge, J. R. Noyes, W. Baumann and M. Beller, *Chem. Commun.*, 2009, 4185–4187.
259 W. Gan, P. J. Dyson and G. Laurenczy, *React. Kinet. Catal. Lett.*, 2009, **98**, 205–213.
260 X. Li, X. Ma, F. Shi and Y. Deng, *ChemSusChem*, 2010, **3**, 71–74.
261 X. Li, F. Shi, X. Ma, L. Lu and Y. Deng, *J. Fuel Chem. Technol.*, 2010, **38**, 544–553.
262 M. E. M. Berger, D. Assenbaum, N. Taccardi, E. Spiecker and P. Wasserscheid, *Green Chem.*, 2011, **13**, 1411–1415.
263 A. Boddien, B. Loges, F. Gärtner, C. Torborg, K. Fumino, H. Junge, R. Ludwig and M. Beller, *J. Am. Chem. Soc.*, 2010, **132**, 8924–8934.
264 A. Boddien, D. Mellmann, F. Gärtner, R. Jackstell, H. Junge, P. J. Dyson, G. Laurenczy, R. Ludwig and M. Beller, *Science*, 2011, **333**, 1733–1736.
265 W. Gan, C. Fellay, P. J. Dyson and G. Laurenczy, *J. Coord. Chem.*, 2010, **63**, 2685–2694.
266 D. J. Morris, G. J. Clarkson and M. Wills, *Organometallics*, 2009, **28**, 4133–4140.
267 M. Czaun, A. Goeppert, R. May, R. Haiges, G. K. S. Prakash and G. A. Olah, *ChemSusChem*, 2011, **4**, 1241–1248.
268 J. D. Scholten, M. H. G. Prechtl and J. Dupont, *ChemCatChem*, 2010, **2**, 1265–1270.
269 S. Enthaler, J. Langermann and T. Schmidt, *Energy Environ. Sci.*, 2010, **3**, 1207–1217.
270 K. Hirota, K. Kuwata and Y. Nakai, *Bull. Chem. Soc. Jpn.*, 1958, **31**, 861–864.
271 Y. K. Sun, J. J. Vajo, C. Y. Chan and W. H. Weinberg, *J. Vac. Sci. Technol., A*, 1988, **6**, 854–855.
272 D. H. S. Ying and R. J. Madix, *J. Catal.*, 1980, **61**, 48–56.
273 N. Aas, Y. Li and M. Bowker, *J. Phys.: Condens. Matter*, 1991, **3**, S281–S286.
274 X. D. Peng and M. A. Barteau, *Catal. Lett.*, 1991, **7**, 395–402.
275 P. A. Dilara and J. M. Vohs, *J. Phys. Chem.*, 1993, **97**, 12919–12923.
276 V. A. Gercher and D. F. Cox, *Surf. Sci.*, 1994, **312**, 106–114.
277 J. Stubenrauch, E. Brosha and J. M. Vohs, *Catal. Today*, 1996, **28**, 431–444.
278 R. Larsson, M. H. Jamroz and M. A. Borowiak, *J. Mol. Catal. A: Chem.*, 1998, **129**, 41–51.
279 G. Y. Popova, T. V. Andrushkevich, Y. A. Chesalov and E. S. Stoyanov, *Kinet. Catal.*, 2000, **41**, 805–811.
280 A. Bandara, J. Kubota and A. Wada, *J. Phys. Chem. B*, 1997, **101**, 361–368.
281 J. Rasko, T. Kecskes and J. Kiss, *J. Catal.*, 2004, **224**, 261–268.
282 T. Shido and Y. Iwasawa, *J. Catal.*, 1993, **141**, 71–81.
283 G. Jacobs, P. M. Patterson, U. M. Graham, A. C. Crawford and B. H. Davis, *Int. J. Hydrogen Energy*, 2005, **30**, 1265–1276.
284 G. Jacobs, P. M. Patterson, U. M. Graham, A. C. Crawford, A. Dozier and B. H. Davis, *J. Catal.*, 2005, **235**, 79–91.
285 Y. Yasaka, H. Yoshida, C. Wakai, N. Matubayasi and M. Nakahar, *J. Phys. Chem. A*, 2006, **110**, 11082–11090.
286 M. Ojeda and E. Iglesia, *Angew. Chem., Int. Ed.*, 2009, **48**, 4800–4803.
287 D. A. Bulusheva, S. Beloshapkin and J. R. H. Ross, *Catal. Today*, 2010, **154**, 7–12.
288 F. Solymosi, Á. Koós, N. Liliom and I. Ugrai, *J. Catal.*, 2011, **279**, 213–219.
289 G. Halasi, G. Schubert and F. Solymosi, *Catal. Lett.*, 2011, **142**, 218–223.
290 D. A. Bulushev, L. Jiaa, S. Beloshapkin and J. R. H. Ross, *Chem. Commun.*, 2012, **48**, 4184–4186.
291 R. Williams, R. S. Crandall and A. Bloom, *Appl. Phys. Lett.*, 1978, **33**, 381–383.
292 H. Wiener, Y. Sasson and J. Blum, *J. Mol. Catal.*, 1986, **35**, 277–284.
293 X. Zhou, Y. Huang, C. Liu, J. Liao, T. Lu and W. Xing, *ChemSusChem*, 2010, **3**, 1379–1382.
294 Y. Huang, X. Zhou, M. Yin, C. Liu and W. Xing, *Chem. Mater.*, 2010, **22**, 5122–5128.
295 S. W. Ting, S. Cheng, K. Y. Tsang, N. van der Laak and K. Y. Chan, *Chem. Commun.*, 2009, 7333–7335.
296 K. Tedsree, T. Li, S. Jones, C. W. A. Chan, K. M. K. Yu, P. A. J. Bagot, E. A. Marquis, G. D. W. Smith and S. C. E. Tsang, *Nat. Nanotechnol.*, 2011, **6**, 302–307.
297 K. Tedsree, C. W. A. Chan, S. Jones, Q. Cuan, W. K. Li, X. Q. Gong and S. C. E. Tsang, *Science*, 2011, **332**, 224–228.
298 X. Gu, Z. H. Lu, H. L. Jiang, T. Akita and Q. Xu, *J. Am. Chem. Soc.*, 2011, **133**, 11822–11825.
299 M. Yadav, T. Akita, N. Tsumori and Q. Xu, *J. Mater. Chem.*, 2012, **22**, 12582–12586.
300 Y. Zhao, L. Deng, S. Ya Tang, D. M. Lai, B. Liao, Y. Fu and Q. X. Guo, *Energy Fuels*, 2011, **25**, 3693–3697.
301 Q. Y. Bi, X. L. Du, Y. M. Liu, Y. Cao, H. Y. He and K. N. Fan, *J. Am. Chem. Soc.*, 2012, **134**, 8926–8933.
302 G. A. Olah, A. Goeppert and G. K. S. Prakash, *Beyond Oil and Gas: The Methanol Economy*, Wiley-VCH, Weinheim, 2006.
303 P. G. Jessop, T. Ikariya and R. Noyori, *Chem. Rev.*, 1995, **95**, 259–272.
304 P. G. Jessop, F. Joó and C.-C. Tai, *Coord. Chem. Rev.*, 2004, **248**, 2425–2442.
305 P. G. Jessop, in *Handbook of Homogeneous Hydrogenation*, ed. J. G. de Vries and C. J. Cornelis, Wiley-VCH, Weinheim, 2007, pp. 489–511.
306 P. Munshi, A. D. Main, J. C. Linehan, C. C. Tai and P. G. Jessop, *J. Am. Chem. Soc.*, 2002, **124**, 7963–7971.
307 J. Elek, L. Nádasdi, G. Papp, G. Laurenczy and F. Joó, *Appl. Catal., A*, 2003, **255**, 59–67.
308 P. G. Jessop, T. Ikariya and R. Noyori, *Nature*, 1994, **368**, 231–233.
309 R. Fornika, H. Görls, B. Seemann and W. Leitner, *J. Chem. Soc., Chem. Commun.*, 1995, 1479–1481.

310 R. Tanaka, M. Yamashita and K. Nozaki, *J. Am. Chem. Soc.*, 2009, **131**, 14168–14169.
311 Y. Himeda, N. Onozawa-Komatsuzaki, H. Sugihara and K. Kasuga, *Organometallics*, 2007, **26**, 702–712.
312 J. F. Hull, Y. Himeda, W. H. Wang, B. Hashiguchi, R. Periana, D. J. Szalda, J. T. Muckerman and E. Fujita, *Nat. Chem.*, 2012, **4**, 383–388.
313 Y. Himeda, *Eur. J. Inorg. Chem.*, 2007, 3927–3941.
314 H. Hayashi, S. Ogo and S. Fukuzumi, *Chem. Commun.*, 2004, 2714–2715.
315 S. Ogo, R. Kabe, H. Hayashi, R. Harada and S. Fukuzumi, *Dalton Trans.*, 2006, 4657–4663.
316 Y. Maenaka, T. Suenobu and S. Fukuzumi, *Energy Environ. Sci.*, 2012, **5**, 7360–7363.
317 G. C. Chinchen, P. J. Denny, J. R. Jennings, M. S. Spencer and K. C. Waugh, *Appl. Catal.*, 1988, **36**, 1–65.
318 A. Kiennemann, J. Idriss, J. P. Hindermann, J. C. Lavalley, A. Vallet, P. Chaumette and P. Courty, *Appl. Catal.*, 1990, **59**, 165–184.
319 M. Bowker, R. A. Hadden, H. Houghton, J. N. Hyland and K. C. Waugh, *J. Catal.*, 1988, **109**, 263–273.
320 P. A. Taylor, P. B. Rasmussen, C. V. Ovesen, P. Stoltze and I. Chorkendorff, *Surf. Sci.*, 1992, **261**, 191–206.
321 H. Nakano, I. Nakamura, T. Fujitani and J. Nakamura, *J. Phys. Chem. B*, 2001, **105**, 1355–1365.
322 M. W. Farlow and H. Adkins, *J. Am. Chem. Soc.*, 1935, **57**, 2222–2223.
323 D. Preti, C. Resta, S. Squarcialupi and G. Fachinetti, *Angew. Chem., Int. Ed.*, 2011, **50**, 12551–12554.
324 H. Wiener, J. Blum, H. Feilchenfeld, Y. Sasson and N. Zalmanov, *J. Catal.*, 1988, **110**, 184–190.
325 Y. Zhang, J. Fei, Y. Yu and X. Zheng, *Catal. Commun.*, 2004, **5**, 643–646.
326 Z. Zhang, Y. Xie, W. Li, S. Hu, J. Song, T. Zhiang and B. Han, *Angew. Chem., Int. Ed.*, 2008, **47**, 1127–1129.
327 T. Inoue, A. Fujishima, S. Konishi and K. Honda, *Nature*, 1979, **277**, 637–638.
328 B. Aurian-Blajeni, M. Halmann and J. Manassen, *Sol. Energy*, 1980, **25**, 165–170.
329 K. R. Thampi, J. Kiwi and M. Grazel, *Nature*, 1987, **327**, 506–508.
330 H. Fujiwara, H. Hosokawa, K. Kurakoshi, Y. Wada, S. Yanagida, T. Okada and H. Kobayashi, *J. Phys. Chem. B*, 1997, **101**, 8270–8278.
331 Y. Amao, *ChemCatChem*, 2011, **3**, 458–474.
332 D. Mandler and I. Willner, *J. Chem. Soc., Perkin Trans. 1*, 1988, **2**, 997–1003.
333 I. Willner and D. Mandler, *J. Am. Chem. Soc.*, 1989, **111**, 1330–1336.
334 I. Willner, N. Lapidot, A. Riklin, R. Kasher, E. Zahavy and E. Katz, *J. Am. Chem. Soc.*, 1994, **116**, 1428–1441.
335 I. Willner, I. Willner and N. Lapidot, *J. Am. Chem. Soc.*, 1990, **112**, 6438–6439.
336 M. Kodaka and Y. Kubota, *J. Chem. Soc., Perkin Trans. 1*, 1999, **2**, 891–894.
337 R. Miyatani and Y. Amao, *Biotechnol. Lett.*, 2002, **24**, 1931–1934.
338 R. Miyatani and Y. Amao, *J. Mol. Catal. B: Enzym.*, 2004, **27**, 121–125.
339 R. Miyatani and Y. Amao, *J. Jpn. Pet. Inst.*, 2004, **47**, 27–31.
340 I. Tsujisho, M. Toyoda and Y. Amao, *Catal. Commun.*, 2006, **7**, 173–176.
341 S. Sato, T. Morikawa, S. Saeki, T. Kajino and T. Motohiro, *Angew. Chem., Int. Ed.*, 2010, **49**, 5101–5105.
342 T. Arai, S. Tajima, S. Sato, K. Uemura, T. Morikawa and T. Kajino, *Chem. Commun.*, 2011, **47**, 12664–12666.
343 S. Sato, T. Arai, T. Morikawa, K. Uemura, T. M. Suzuki, H. Tanaka and T. Kajino, *J. Am. Chem. Soc.*, 2011, **133**, 15240–15243.
344 T. Arai, S. Sato, K. Uemura, T. Morikawa, T. Kajino and T. Motohiro, *Chem. Commun.*, 2010, **46**, 6944–6946.
345 T. M. Suzuki, H. Tanaka, T. Morikawa, M. Iwaki, S. Sato, S. Saeki, M. Inoue, T. Kajino and T. Motohiro, *Chem. Commun.*, 2011, **47**, 8673–8675.
346 R. P. Linstead and S. L. S. Thomas, *J. Chem. Soc.*, 1940, 1127–1134.
347 N. F. Grunenfelder and T. H. Schucan, *Int. J. Hydrogen Energy*, 1989, **14**, 579–586.
348 J. K. Ali, E. J. Newson and D. W. T. Rippin, *Chem. Eng. Sci.*, 1994, **13**, 2129–2134.
349 N. Meng, S. Shinoda and Y. Saito, *Int. J. Hydrogen Energy*, 1997, **22**, 361–367.
350 C. M. Jensen, *Proceedings of the U.S. DOE Hydrogen Program Review*, Herndon, VA, 1997.
351 S. Hodoshima, S. Takaiwa, A. Shono, K. Satoh and Y. Saito, *Appl. Catal., A*, 2005, **282**, 235–242.
352 G. P. Pez, A. Scott, A. Cooper and H. Cheng, *US Pat.*, 7101530, 2006.
353 A. Cooper and G. P. Pez, *Proceedings of the US DOE hydrogen Program review*, Crystal City, VA, 2006.
354 D. E. Schwarz, T. M. Cameron, P. J. Hay, B. L. Scott, W. Tumas and D. L. Thorn, *Chem. Commun.*, 2005, 5919–5921.
355 Y. Okada, E. Sasaki, E. Watanabe, S. Hyodo and H. Nishijima, *Int. J. Hydrogen Energy*, 2006, **31**, 1348–1356.
356 A. Moores, M. Poyatos, Y. Luo and R. H. Crabtree, *New J. Chem.*, 2006, **30**, 1675–1678.
357 R. B. Biniwalea, S. Rayalua, S. Devottaa and M. Ichikawab, *Int. J. Hydrogen Energy*, 2008, **33**, 360–365.
358 R. H. Crabtree, *Energy Environ. Sci.*, 2008, **1**, 134–138.
359 Y. Cui, S. Kwok, A. Bucholtz, B. Davis, R. A. Whitney and P. G. Jessop, *New J. Chem.*, 2008, **32**, 1027–1037.
360 D. Teichmann, W. Arlt, P. Wasserscheid and R. Freymann, *Energy Environ. Sci.*, 2011, **4**, 2767–2773.